TRACING TRANSCONTINENTAL SAND TRANSPORT: FROM ANATOLIA-ZAGROS TO THE RUB' AL KHALI SAND SEA

EDUARDO GARZANTI[1*], PIETER VERMEESCH[2], KHALID ABDULSAMAD AL-RAMADAN[3], SERGIO ANDÒ[1], MARA LIMONTA[1], MARTIN RITTNER[2], GIOVANNI VEZZOLI[1]

[1] Laboratory for Provenance Studies, Department of Earth and Environmental Sciences, University of Milano-Bicocca, 20126 Milano, Italy

[2] London Geochronology Centre, Department of Earth Sciences, University College London, London, WC1E 6BT, UK

[3] King Fahd University of Petroleum & Minerals, Dhahran, 31261 Saudi Arabia.

* Corresponding author. Tel.: +39-02-64482088; fax: +39-02-64482073.

E-mail addresses: eduardo.garzanti@unimib.it (E. Garzanti), p.vermeesch@ucl.ac.uk (P.Vermeesch), ramadank@kfupm.edu.sa (K.A. Al-Ramadan), sergio.ando@unimib.it (S. Andò), mara.limonta@unimib.it (M.Limonta), m.rittner@ucl.ac.uk (M.Rittner), giovanni.vezzoli@unimib.it (G. Vezzoli),

[1] Tel.: +39-02-64482088; fax: +39-02-64482073
[2] Tel.: +44-020-76792418; fax: +44-020-76792867
[3] Tel: +966-3-8607175

KEY WORDS: Sand petrography; Heavy minerals; U-Pb zircon geochronology; Sediment dispersal pathways; Intrasample mineralogical variability; Mineral durability during eolian transport.

ABSTRACT

We used petrographic, heavy-mineral and geochronological signatures of sand-sized grains to document an exceptional case of long-distance sediment transport dominated by eolian processes in hyperarid climate. Feldspatho-quartzo-lithic orogenic detritus shed by the Anatolia Plateau and Zagros Mountains - including carbonate, chert, volcanic, metabasite and ultramafic lithic grains with a rich epidote-amphibole-pyroxene-garnet heavy-mineral suite - was carried to the Arabian-Gulf foreland basin via the Euphrates-Tigris-Karun fluvial system and other rivers draining the Zagros, and blown inland by dominant Shamal winds to reach well into the Arabian foreland. Sediment dispersal over a cumulative distance of up to 4000 km took place in multiple steps, involving extensive eolian reworking of older deposits during lowstand stages of the Pleistocene before final accumulation in the Rub' al Khali sand sea. The siliciclastic fraction of Gulf beaches changes southeastwards from litho-quartzose carbonaticlastic and quartzose north of Qatar to quartzo-lithic carbonaticlastic along the Trucial Coast, but invariably contains chert, volcanic and metabasite lithics, together with epidote, pyroxene, amphibole, and garnet. Dune sand inland is progressively enriched in quartz until composition becomes feldspatho-quartzose, whereas the heavy-mineral assemblage remains virtually unchanged. Beach and dune sands of the Gulf and northeastern Rub' al Khali were derived from Arabia, Anatolia and the Zagros in varying proportions, with only local contribution from ophiolites of the northern Oman Mountains as revealed by cellular serpentinite and enstatite grains. In all samples detrital zircons yielded mostly Cambrian to Neoproterozoic ages reflecting "Pan-African" crustal growth and amalgamation of the Arabian shield, but several Upper Paleozoic, Mesozoic, and Cenozoic zircons with ages as young as 5 Ma in northeastern Rub' al Khali dunes document ultimate provenance from the Anatolia-Zagros orogen. Quartzose dune sand of the southwestern Rub' al Khali, containing a moderately poor, amphibole-rich heavy-mineral assemblage and very few young zircons, is dominantly Arabian-derived. Relatively soft carbonate grains are typically concentrated in finer sand classes, which is ascribed to both mixing with coarser quartz recycled from Arabian siliciclastic covers and selective

mechanical wear during multicyclic long-distance transport in high-energy eolian environments. Understanding the complex transfer of huge detrital masses on the Earth's surface, and mixing of sediments derived from different sources along successive tracts of a composite routing system that may cover cumulative distances of thousands of kilometers across climatic and tectonic boundaries over time periods of millions of years, is essential to enhance the resolution of source-to-sink studies and avoid gross oversimplifications in paleogeographic reconstructions.

> "Realistic concepts about provenance relations require attention to the variability and complexity of sediment dispersal systems on a dynamic earth."
> *Dickinson 1988*

> "You have not awakened to wakefulness, but to a prior dream. This dream is enclosed within another, and so on to infinity, which is the number of grains of sand. The path you must retrace is interminable and you will die before you have truly awakened."
> *Jorge Luis Borges, La escritura del dios, El Aleph, 1949*

INTRODUCTION

A great challenge to provenance studies is posed by the variability of source-to sink dispersal paths, which may involve diverse configurations of fluvial, eolian, shallow-marine or deep-marine tracts, each extending over several hundreds or even thousands of kilometers in length (Dickinson 1988). A common case is that of coupled fluvial and turbiditic transport, in which sediment generated in high mountain ranges is carried by gravity-driven currents along a winding route to the coast and next across the continental shelf and slope to eventually reach the abyssal ocean floor (Zuffa et al. 2000; Ingersoll et al. 2003; Limonta et al. 2015). Less commonly documented is long-distance transport in littoral environments alongshore and onshore, where sand blown by dominant winds can climb up to a thousand meters uphill over a distance of hundreds of kilometers inland (Garzanti et al. 2012a, 2014).

The complexities of ultra-long sediment-routing systems can be unraveled in full detail only by the use of complementary provenance techniques in modern settings, where we can gain complete knowledge on the topography, areal extent, lithology and tectonic structure of source terranes, as well as on climatic conditions including atmospheric and oceanic circulation patterns. In this article we use petrographic, heavy-mineral and geochronological signatures of sand-sized grains to monitor sediment transfer along the southern coast of the Arabian Gulf, and beyond it toward the heart of the huge Rub' al Khali sand sea (Fig. 1). The present article is based on, and represents the continuation of two provenance studies on eolian and fluvial sands of northern Arabia and the Euphrates-Tigris-Karun rivers (Garzanti et al. 2013, 2016), which allowed us to determine accurately the composition of sediments derived and transported from both the Arabian foreland and the Anatolia-Zagros orogen to the Mesopotamian-Gulf foreland basin. We can thus document a remarkable case of multi-step sediment transfer over a distance of thousands of kilometers, characterized by repeated recycling throughout the Quaternary and dominated by eolian processes in hyperarid climatic conditions.

ARABIA AND THE GULF

Geology

The Arabian plate is delimited by the Bitlis-Zagros convergent plate boundary in the north and north-east, and by the Levant-Red Sea-Gulf of Aden divergent plate boundary in the west and south. A central shield, generated during Neoproterozoic accretion of continental microplates and arc terranes (Johnson et al. 2011), tilted gently toward the Gulf, is overlain by a semicircular belt of eastward-younging Paleozoic to Cenozoic siliciclastic to shallow-marine carbonate strata (Fig. 2; Alsharhan and Nairn 1997; Cantrell et al. 2014).

Strong weathering and erosion followed the Neoproterozoic ("Pan-African") orogeny, when the region became a vast low-relief surface upon which Lower Paleozoic sandstones were deposited non-conformably (Avigad et al. 2005). The thick succession exposed on the Wajid Plateau south of the central shield, consisting of fluvio-glacial to shallow-marine conglomerates and quartzose sandstones with locally interbedded mudrocks, has been subdivided into several formations separated by unconformities and ranging in age from the Cambro-Ordovician to the early Permian (Al-Ajmi et al. 2015). Outcrops of Permian limestones and Triassic strata are limited in the area. The Jurassic succession exposed in Jabal Tuwaiq (*jabal* = mountain) consists of shallow-marine carbonates, intercalated with shales and sandstones at the base and capped by evaporites. A thick succession of Paleogene carbonates and evaporites overlying deltaic to shallow-marine quartzose sandstones of Cretaceous age is exposed in the Hadhramaut carbonate tableland sloping gently northward toward the Rub' al Khali. Weakly metamorphosed Neoproterozoic to Lower Paleozoic strata and overlying Tethyan carbonates of the Arabian platform crop out in the Huqf arch to the north-east, and within tectonic windows in the northern Oman Mountains farther north (Glennie et al. 1974). Mesozoic carbonates are also exposed in the Musandam Peninsula, representing the eastern termination of the Zagros thrust belt (Searle et al. 1983). The Sama'il Ophiolite, spectacularly exposed along an arcuate belt ~500 km long in northern Oman, includes 8-12 km-thick serpentinized mantle harzburgites, 3–6 km-thick gabbros with ultramafic cumulates at the base and plagiogranite pockets at the top, 1–1.5 km-thick diabase sheeted dikes, and 0.5–2 km-thick pillow basalts overlain by thin metalliferous strata and radiolarites (Lippard et al. 1986). Tectonically imbricated beneath the ophiolite are Permo-Mesozoic radiolarian cherts and limestone turbidites well exposed along the southern front of the orogen (Hawasina thrust sheets; Béchennec et al. 1990).

Wind regimes

Arabia lies within the trade-wind belt of the Northern Hemisphere. Winds travel from the Mediterranean Sea toward the Gulf, and next turn to the south and southwest toward the core of the Rub' al Khali (Fig. 3). Northwesterly winds blow in early winter and late spring. Maximum release of eolian energy is in June to early July, when Shamal (*shamal* = north) wind may last for weeks with speeds of 40–50 km/h and gusts up to 100 km/h. Dust storms are generated during the day, whereas wind calms down at night. Sand is deflated in the higher-energy area north of Dammam and transported actively southward across the Jafurah Sand Sea (Fig. 1; Fryberger et al. 1984). Wind energy declines steadily southward and westward across the Rub' al Khali, where rare sandstorms occur (Vincent 2008 p.135-137). The southwesterly monsoon (*mawsim* = season), a humid summer wind bringing gusts up to 100 km/h and rough seas along the coast of southeastern

Arabia, blows in the opposite direction, with a branch swinging northward across the Wahiba Sands toward the Oman Mountains (Glennie and Singhvi 2002).

Dune fields

The active dune fields of Arabia represent the largest continuous body of eolian sand on Earth (Fig. 2). Sand accumulates in the Great Nafud to the north and in the Rub' al Khali to the south, connected by sub-parallel arcuate corridors of mobile reddish dunes running from north to south along topographic depressions delimited by resistant strata (e.g. Jurassic limestone of Jabal Tuwaiq). The Nafud corridors (*nafud* = sandy desert) run at elevations ≥700 m a.s.l. west of Jabal Tuwaiq, whereas the Ad Dahna corridor swings east of it in a 1200 km-long by 30-80 km-wide arc at elevations declining southward from 560 to 300 m a.s.l.. Mobile barchans of light brown sand characterize the Jafurah sand sea, starting north of Dammam and widening southward along the Gulf coast to finally merge into the Rub' al Khali.

The Rub' al Khali (or *Empty Quarter*, known locally as *Ar Ramlah* = The Sands) occupies the ~600,000 km^2 wide rim basin behind the rift shoulders of the Red Sea and Gulf of Aden, with slopes decreasing steadily from ~1200 m a.s.l. to the Trucial Coast of the United Arab Emirates (UAE). Potential evaporation exceeds precipitation by factors of 10 to 30, rainfall is < 60 mm/year, and summer temperatures > 50°C. Linear dunes are up to 250 km-long, 1.5 km-wide, 200 m-high, and spaced from 2 to 6 km apart; star dunes are up to 300 m-high (Vincent 2008 p.138-144). Compound mega-barchans up to 160 m-high migrate slowly landward at its upwind northeasternmost edge at Liwa (Goudie et al. 2000; Stokes and Bray 2005; Bishop 2013; Farrant et al. 2015). Seif dunes extend toward Oman with WNW–ESE-trending axes, whereas a branch is deflected northward along the front of the northern Oman mountains towards the Musandam Peninsula. In eastern Oman lie the coastal Wahiba Sands, where northward sand transport took place mostly during Pleistocene eustatic lowstands (Radies et al. 2004). The Rub' al Khali is delimited to the south by the Hadhramaut-Dhofar Arch, surrounded by locally fed dune fields (e.g., Ramlat as Sab'atayn in Yemen; Garzanti et al. 2001).

The Gulf

The Arabian (Persian) Gulf is the distal underfilled part of the Zagros foreland basin (Evans 2011). Given the dry hot climate of the region, carbonate sedimentation flourishes along the Arabian coast, fringed by coral reefs, tidal flats, barrier islands and lagoons, ooidal shoals, beaches and *sibakh* (*sabkhah* = flat dry salt-encrusted zone; Kendall and Alsharhan 2011). Carbonaticlastic terrigenous detritus derived from the Shatt al Arab estuary and from the Zagros Mountains along the opposite side, is however also significant (Baltzer and Purser 1990; Walkden and Williams 1998).

From Kuwait to Qatar, offshore winds supply quartzose sand that mixes and intercalates with shallow-marine carbonates (Fryberger et al. 1983) Coastal features are structurally controlled, with cuspate spits forming on structural highs whereas intervening embayments are infilled by beach-ridge and sabkha sediments (Lomando 1999). The Trucial (Pirate) Coast of the UAE receives no runoff from interior Arabia and most of the Oman Mountains. Water depths offshore are < 20 m and numerous islands lie atop salt domes and the Great Pearl Bank, the eolianite-cored peripheral bulge joining the coast at low angle north of Abu Dhabi (Farrant et al. 2012). Skeletal sands, including red algae from adjacent reefs, are deposited on high-energy shorelines, replaced by pellets and compound grains in sheltered areas. Tidal range of 1–2 m and current velocities up to 65 cm/s within tidal channels favour development of oolitic ebb-tide deltas. Ooids form in open tidal flats and lagoons, where salinity reaches 50–70‰. Storm beaches backed by coastal dunes and several spits indicating northeastward longshore transport characterize the linear eastern coast, which is exposed obliquely to Shamal winds in the direction of the longest fetch (Purser 1973; Kendall and Alsharhan 2011).

The Gulf was largely emergent during a significant part of the Quaternary. Its notably flat floor, exposed extensively whenever sea-level fell below -70 m during glacial periods, was entirely subaerial during the Late Glacial Maximum when sea level dropped to -120 m (Glennie 1998). The Tigris-Euphrates paleoriver then extended across lake-dotted marshlands all the way to the Straits of Hormuz, where its entrenched channel debouched directly into the Gulf of Oman (Uchupi et al. 1999). The potential for wind deflation by northwesterly Shamal winds would have been greatest during early regressive stages, when the unconsolidated sediments newly exposed by the receding sea were not yet stabilised by vegetative cover or early cementation (Alsharhan and Kendall 2003). Sea level returned to rise after the Late Glacial Maximum, when marine waters transgressed back through the Straits of Hormuz, progressively drowning the lower reaches of the extended Tigris-Euphrates paleoriver and thus permanently eliminating floodplain sediments as a source of eolian sand (Lambeck 1996).

Relict Pleistocene paleodunes are exposed widely along the Gulf coast and in deflated areas as far as 80 km inland (Williams and Walkden 2002). Moderately to well cemented, polyphase carbonate-rich eolianites are underlain by siliciclastic paleodunes, resting disconformably in turn on the Upper Miocene Baynunah Formation (Glennie and Singhvi 2002; Farrant et al. 2015). Baynunah sediments rich in vertebrate fossils were deposited by a large fluvial system flowing constantly from the west-north-west, possibly the Tigris-Euphrates paleoriver (Friend 1999; Hill et al. 2012). A major drainage system also existed in central Arabia at wetter times, including an ancestral Wadi Sahba, possibly joined by Wadi Dawasir (Al-Saad et al. 2002; fig. 6.5 in Edgell 2006; Bibi et al. 2013).

METHODS

During the field campaigns organized in Saudi Arabia by the King Fahd University in October 2014 and May 2016, we have collected 7 beach and 1 dune sands along the Gulf coast from Kuwait to

Dammam, 19 dune sands in the northeastern Rub' al Khali along a NW-SE transect from west of Sabkha Matti to Shaybah, Ardah and the Oman border, and 12 dunes and 2 sand sheets in the southwestern Rub' al Khali (Fig. 1). For consistency and to avoid anomalous concentrations of denser minerals due to wind turbulence along the flanks and stoss side of dunes, all samples were taken from the crest at the top of the largest dune in each site. We also collected 1 gravel sample from the alluvial fan-apron fed from the northern Oman Mountains, 10 sands on the bed of major widyan (*wadi* = "dry valley") feeding into the southwestern Rub' al Khali, and one bedrock sample from the Paleozoic Wajid Sandstone. These 52 samples integrate those studied in previous years, covering fluvial systems of Mesopotamia, beaches along the southern coast of the Gulf, and rivers and dune fields of northern Arabia, Oman and Yemen (Garzanti et al. 2001, 2003, 2013, 2016). Full information on sampling sites is provided in Appendix Table A1 and Google-Earth™ map *Arabia&Gulf.kmz*.

Sand petrography and heavy minerals

A quartered fraction of each sand sample was impregnated with Araldite, cut into a standard thin section stained with alizarine red to distinguish dolomite and calcite, and analysed by counting 400 points under the microscope (Gazzi-Dickinson method; Ingersoll et al. 1984; Zuffa 1985). Wadi samples were gently washed to remove mud or wet sieved to obtain the 63-2000 μm class if poorly sorted and containing granules. Sand classification is based on the main components quartz, feldspars and lithic fragments considered if exceeding 10%QFL (e.g., a sand is named litho-feldspatho-quartzose if Q>F>L>10%QFL; Garzanti 2016). Metamorphic rock fragments were subdivided into very low to low-rank metasedimentary or metavolcanic, and medium to high-rank felsic or mafic categories (Garzanti and Vezzoli 2003). Criteria for distinguishing the intrabasinal versus extrabasinal origin of calcareous and other grains are after Zuffa (1985) and Garzanti (1991). Median grain size was determined in thin section by ranking sand samples from coarsest to finest followed by visual comparison with in-house standards sieved at 0.25 □ sieve interval. Heavy-mineral analyses were carried out in bulk for well sorted dune samples, and on the <500 µm, 15-500 µm or 32-500 µm fraction obtained by wet sieving for less sorted wadi, beach, and sand-sheet samples. Heavy minerals were separated by centrifuging in Na polytungstate (density ~2.90 g/cm^3), recovered after partial freezing of the test tube with liquid nitrogen. The obtained fraction was weighted, micro-quartered, and mounted on a glass slide with Canada balsam for counting. In order to obtain real volume percentages, about 200 transparent heavy minerals were point-counted under the microscope at a regular spacing wide enough to avoid counting the same grain twice (Galehouse 1971). Altered and dubiously identified grains were checked by Raman spectroscopy (Andò and Garzanti 2014). Heavy-mineral concentration, calculated as the volume percentage of total (HMC) and transparent (tHMC) heavy minerals (Garzanti and Andò 2007), ranges from extremely poor ($HMC < 0.1$) and poor ($0.5 \leq HMC < 1$) to rich ($5 \leq HMC < 10$) and very rich ($10 \leq HMC < 20$). The ZTR index (sum of zircon, tourmaline and rutile over total transparent heavy minerals; Hubert 1962) expresses the "mineralogical durability" of the suite (Garzanti 2017). Detrital components are listed in order of abundance throughout the text. Key parameters are shown in Table 1; the complete petrographic and heavy-mineral datasets are provided in Appendix Tables A2 and A3.

Detrital geochronology

Detrital zircons were identified by QEMScan electron microscopy (Vermeesch et al. 2017) on the heavy-mineral separates of 27 selected sand samples from Saudi Arabia (32-500 µm class for wadi and beach sands, bulk sample for well sorted dune sands). U-Pb zircon ages were determined at the London Geochronology Centre using an Agilent 7700x LA-ICP-MS system, employing a NewWave NWR193 Excimer Laser operated at 10 Hz with a 20 µm spot size and ~2.5 J/cm^2 fluence. To treat all samples equally and avoid intersample bias, the laser spot was always placed "blindly" in the middle of zircon grains. We deliberately decided not to image the grains, because this may introduce bias. One of the advantages of the QEMScan is that all zircons are picked, including murky grains easily discarded by visual inspection but invariably confirmed to be zircon by LA-ICP-MS analysis. Data reduction was performed using GLITTER 4.4.2 software (Griffin et al. 2008). We used $^{206}Pb/^{238}U$ and $^{207}Pb/^{206}Pb$ ages for zircons younger and older than 1100 Ma, respectively. No common Pb correction was applied (for further methodological information see supplementary material in Rittner et al. 2016). Grains with > +5/-15% age discordance were discarded, and 2812 concordant ages were obtained overall (> 100 ages on 17/27 samples). Statistical techniques used for data presentation include kernel density estimation (Vermeesch 2012) and multidimensional scaling, which produces "maps" in which samples are arranged according to their statistical distance (Vermeesch 2013). The full geochronological dataset is provided in Appendix B.

DETRITAL SIGNATURES

In this section we illustrate sand composition in beaches along the Arabian coast of the Gulf and in dune fields inland (Fig. 4 and 5). Descriptions are integrated with data on wadi sands and on beach and dune sands collected in previous years (Table 1).

Beaches of the Arabian Gulf

Along the Gulf coast, terrigenous siliciclastic and subordinately carbonaticlastic detritus mixes in various proportions with a locally overwhelming allochemical (coeval) to extrasequential (non-coeval) intrabasinal fraction represented by ooids with subordinate bioclasts (pelecypods, gastropods, benthic and very rarely planktonic foraminifera) and fragments of calcite-cemented eolianite, beachrock, or calcrete crusts. Quartz and other terrigenous grains commonly show ooidal rims; glaucony also occurs.

Beach sand from Kuwait to Qatar ranges from feldspatho-litho-quartzose to quartzose (Fig. 4A). North of Dammam, feldspatho-litho-quartzose to litho-quartzose carbonaticlastic sand has plagioclase/total feldspar ratio (P/F) up to 0.68, more common volcanic, chert and metabasite lithics, and very poor to poor heavy-mineral suite with ZTR <10, abundant epidote, common clinopyroxene, garnet and amphibole, and minor hypersthene, Cr-spinel, titanite, staurolite and enstatite. South of Dammam, feldspatho-quartzose to quartzose sand has P/F ≤ 0.25 and extremely poor to very poor suite with ZTR commonly reaching ~30.

Along the Trucial Coast of the UAE, beach sand is quartzo-lithic carbonaticlastic with P/F 0.60±0.15 and common chert, mainly mafic volcanic, metabasite and siltstone/metasiltstones grains. The mainly poor heavy-mineral suite includes abundant epidote associated with amphibole, garnet and clinopyroxene, low ZTR (3±2), and minor Cr-spinel. Cellular serpentinite grains and enstatite are more common close to the Oman Mountains in the south-east.

Coastal dune fields

In Saudi Arabia, sparse dunes north of Dammam - where winds are stronger and deflation prevails (Fryberger et al. 1984) - are quartzose with minor feldspars (P/F 0.41), mainly carbonate rock fragments, and a poor epidote-amphibole-clinopyroxene-garnet heavy-mineral suite (ZTR 5). Coastal Jafurah dunes south of Dammam are litho-feldspatho-quartzose (P/F 0.31±0.13) with poor to moderately poor epidote-clinopyroxene-amphibole-garnet suites (ZTR 8±3). Dunes in Niqyan Qatar and just south of the Qatar border are feldspatho-litho-quartzose (P/F 0.51±0.03), with moderately poor clinopyroxene-amphibole-garnet-epidote or extremely poor epidote-dominated suites (ZTR 5±2). Carbonate and subordinate volcanic, low-rank metasedimentary, metabasite and chert lithics are concentrated in the fine tail of the size distribution (fig.7 in Garzanti et al. 2013). Jafurah dunes inland are instead quartzose, with low P/F (0.17±0.05) and very poor amphibole-epidote-clinopyroxene-garnet suites with high ZTR (14±9).

Dune sand composition varies more markedly landward in the UAE (Pugh 1997; Hadley et al. 1998; Teller et al. 2000), where quartzo-lithic carbonaticlastic sand of creamy yellow coastal dunes passes inland to feldspatho-litho-quartzose and eventually litho-feldspatho-quartzose sand of reddish barchanoid megadunes in the Liwa oasis. Feldspars increase landward slower than quartz, with rather constant P/F (0.48±0.11). Chert grains are more common than volcanic and metabasite grains. Serpentinite grains increase notably toward the Oman Mountains. Poor heavy-mineral suites include mainly epidote associated with amphibole, garnet, and minor clinopyroxene and enstatite; ZTR increases inland from 1 to 5-10.

The northeastern Rub' al Khali

Dune sands inland of Sabkha Matti are feldspatho-litho-quartzose to feldspatho-quartzo-lithic carbonaticlastic (Fig. 4B; P/F 0.54±0.06) with a varied lithic population and poor to moderately poor epidote-amphibole-clinopyroxene-garnet heavy-mineral suites (ZTR 5±2). Megadunes in the Shaybah area are feldspatho-quartzose (Fig. 4C; P/F 0.55±0.06), with a very poor to poor epidote-amphibole-garnet-clinopyroxene suite (ZTR 6±4). Dunes in the Ardah area are similarly feldspatho-quartzose (Fig. 4F; P/F 0.48±0.12) with mainly very poor epidote-amphibole-garnet-clinopyroxene suites (ZTR 7±2), but may contain common carbonate grains concentrated in the fine tail of the size distribution (Fig. 4E). Anomalous concentration of ultrandense opaque Fe-Ti-Cr oxides and zircon (HMC up to 14) is induced locally by wind deflation on dune flanks.

The southwestern Rub' al Khali

Sand sheets and dunes along the western edge of the Rub' al Khali range from feldspatho-quartzose to quartzose (P/F 0.52±0.13). Limestone grains may be concentrated in the fine tail of the size distribution together with a few siltstone/metasiltstone, metabasite, felsic metamorphic, volcanic/metavolcanic, dolostone, chert, and shale/slate grains. Heavy-mineral suites are moderately rich in sand sheet and dune sands at the northern and western edges of the desert, and become mainly poor eastward into the sand sea (McClure 1984 p.102). Amphibole dominates over epidote; zircon, garnet and clinopyroxene are minor, and staurolite, enstatite and hypersthene rare (ZTR 7±4).

Arabian widyan

Because of arid to hyperarid climate all Arabian rivers are ephemeral (*widyan* = dry valleys). During more humid Pleistocene stages, however, major rivers now clogged by eolian sand were capable of flowing to the Gulf (Edgell 2006). One was the Wadi Rimah-Wadi al Batin system, which in rushing floods carried rock debris eroded from crystalline uplands of the Arabian shield, cut steep-walled canyons through limestone plateaus, and finally spread out and dropped its load to form a large alluvial fan, now the gently sloping Dibdiba deflated gravel plain between southern Iraq and Kuwait (Holm 1960; Al-Sulaimi and Pitty 1995). Sand in Wadi Rimah and Wadi al Batin is quartzose. The very poor heavy-mineral suite consists of a largely eolian coarser fraction rich in zircon, tourmaline and rutile, with a fluvial finer fraction rich in amphibole and clinopyroxene (ZTR 41-42), indicating extensive mixing with eolian sand across Nafud and Dahna dune corridors.

In central Arabia, Wadi Sahba drains the Tuwaiq limestone plateau and once ran eastward to Harad (Anton 1983), from where a series of divergent gravel trains fan out toward Sabkha Matti (fig. 6.6 in Edgell 2006). Sand in Wadi Sahba and in other streams also draining Jabal Tuwaiq (Wadi Ushayrab, Maqran, and Sulayyil) is quartzo-lithic carbonaticlastic with a very poor amphibole-rich heavy-mineral suite including common epidote, and minor zircon, clinopyroxene, tourmaline and rutile (Fig. 5A; ZTR 16±9).

Wadi ad Dawasir once deposited a broad gravel plain now largely covered by Rub' al Khali dunes. Fine sand is litho-quartzose carbonaticlastic whereas medium sand is feldspatho-litho-quartzose (P/F 0.65±0.12), revealing mixed provenance from the Arabian shield and its Paleozoic to Jurassic cover strata (Fig. 5B). The moderately poor, hornblende-dominated suite includes common epidote, and minor zircon and clinopyroxene (ZTR 4±1).

In southwestern Arabia, Wadi Hubuna and Wadi Qatan drain the Arabian shield and carry feldspatho-quartzose metamorphiclastic/plutoniclastic sand (Fig. 5C; P/F 0.68±0.25) with a moderately rich to very rich hornblende-epidote suite including clinopyroxene and minor garnet and hypersthene (ZTR 2±2). Wadi Hima and Wadi Najran, draining exclusively and in part Paleozoic sandstones respectively, carry virtually purely quartzose and quartzose sand with very poor and moderately poor amphibole-dominated suites including epidote, clinopyroxene, garnet, hypersthene, and locally olivine (Fig. 5D; ZTR 3±1). The Paleozoic Wajid Sandstone is quartzose with a few feldspars (Fig. 5E; P/F 0.63) and an extremely poor heavy-mineral suite with high ZTR (54) including a few garnet, staurolite and amphibole grains.

Omani and UAE widyan

Wadi Kabir and Wadi Sumaini draining the southwestern flank of the northern Oman mountains carry lithic ultramaficlastic sand with rich to very rich enstatite-olivine or epidote-amphibole-enstatite suites also including clinopyroxene and hypersthene. Wadi Ghub and Wadi Dhaid in the eastern UAE carry quartzo-lithic sedimentaclastic sand with moderately rich to very rich epidote-clinopyroxene-amphibole suites including enstatite, garnet, hypersthene, olivine, and Cr-spinel. Wadi Bih draining the Musandam peninsula carries almost purely carbonaticlastic lithic sand.

INTRASAMPLE COMPOSITIONAL VARIABILITY

Intrasample compositional variability is primarily a settling-equivalence effect (Rubey 1933), dense and ultradense detrital components being progressively and systematically enriched in finer classes of the size distribution (Fig. 6; see Garzanti et al. 2008 for detailed quantification of size-density sorting effects). Exceptions to the rule may reveal mixing of detrital populations with different provenance and grain size, providing key information for a refined textural interpretation and provenance analysis (e.g., Garzanti et al. 2015).

Framework petrography

For ten dune samples, five each for the northeastern and southwestern Rub' al Khali, data were obtained by point-counting in thin section by using separate sheets for grains of fine, medium, and coarse sand size measured by an ocular micrometer applied to the microscope (Fig. 6A,B). In light-cream dunes inland of Sabkha Matti, plagioclase prevails over K-feldspar with P/F ratio decreasing markedly with grain size. Abundant limestone and dolostone grains are associated with chert, metasedimentary, metavolcanic and volcanic lithics in the fine class, whereas the coarse class consists dominantly of mainly rounded quartz (Fig. 4B). Such a notable concentration of plagioclase and lithic grains in the fine class cannot be ascribed to either size-density sorting or selective abrasion, because these grains are as dense or only a little denser than quartz, and some (e.g., chert) are even more resistant than monocrystalline quartz to mechanical wear (Harrell and Blatt 1978; McBride and Picard 1987 p.1025). Provenance control is thus revealed.

In the Shaybah and Ardah areas, all lithic fragments decrease toward the heart of the Uruq al Mutaridah (*uruq* = linear dunes) because of mixing in larger proportions with quartzose detritus derived from Arabian sources (Fig. 4). But carbonate grains decrease in abundance and size faster than tougher chert grains (Fig. 7), and are commonly observed to concentrate markedly in the fine tail of the size distribution just before they finally disappear downwind (Fig. 4B,E). Size reduction and roundability of carbonate grains by mechanical wear has been documented already a century ago (Wentworth 1919). Otherwise detrital modes do not show marked grain-size control, and feldspars tend to increase slightly in the coarse sand class, with rather constant P/F.

In dunes and sand sheets of the southwestern Rub' al Khali, feldspars and lithic grains (carbonate and subordinately metavolcanic, metasedimentary, chert, siltstone, metabasite) are markedly concentrated in the fine class, where K-feldspar and plagioclase are equally abundant (P/F 0.45±0.05). Quartz increases in coarser classes, where K-feldspar prevails (P/F 0.28±0.11). Mixing of quartz-rich sand recycled from mostly Paleozoic quartzose sandstones with finer detritus derived from the Arabian shield and Mesozoic sedimentary covers is indicated.

Heavy minerals

Intrasample variability was investigated in detail for the Taroot beach and the Tamani dune samples, which were sieve-split into 0.25 □ subclasses. Seven subclasses between 80 and 300 µm for the Taroot beach, representing 81% of the bulk sample in weight and 98% of the total dense fraction, and nine subclasses between 63 and 300 µm for the Tamani dune, representing 95% of the bulk sample and 99.5% of the total dense fraction, were analysed separately (Fig. 6C).

In the Taroot sample, heavy-mineral and transparent-heavy-mineral concentrations decrease systematically from 16 and 11 in the finest analysed subclass, where ultradense monazite was recorded and zircon is most common, to 0.11 and 0.04 in the coarsest analysed subclass, where low-density tourmaline and andalusite reach maximum. Not all minerals, however, conform to the settling-equivalence principle. Relatively low-density pyroxene is most abundant in the finest subclass, and together with garnet and amphibole reaches a relative minimum in the modal subclass, where epidote, largely hosted within rock fragments, reaches maximum.

In the Tamani sample, the HMC and tHMC indices also decrease systematically from the finest (17 and 14) to the coarsest analysed subclasses (0.13 and 0.03). Ultradense minerals, however, do not reach their relative maximum in the finest subclass but in the 106-125 µm (opaque Fe-Ti-Cr oxides), 125-150 µm (zircon, rutile) or 150-180 µm (garnet) subclasses. Epidote, staurolite, and less regularly garnet unexpectedly increase progressively with grain size relative to lower-density amphibole.

Anomalies in size-density relationships can be investigated by settling-equivalence analysis (Garzanti et al. 2008), which indicates that the settling-equivalence principle accounts for no more than a fifth and a third of intrasample variability in the Taroot and Tamani samples, respectively. In both samples, size shifts (i.e., differences between the size of a given mineral and bulk-sample grain size measured in □ units) do not increase progressively from less dense to ultradense heavy minerals as theoretically predicted, and are similar or even higher for clinopyroxene than for zircon (0.57□ vs. 0.55□ for Taroot beach, 0.42□ vs. 0.35□ for Tamani dune, respectively). This indicates mixing of zircon-bearing and virtually pyroxene-free quartzose sand recycled from Arabian siliciclastic covers with a nearly half-□-class finer, pyroxene-bearing detrital population. In the Taroot beach such a population is characterized by a distinct Mesopotamian (i.e., Tigris + Euphrates) signature, whereas in the Tamani dune it is derived largely from the outer flank of the Red Sea rift shoulder although possibly in minor part even ultimately long-distance from the Anatolia-Zagros orogen. Most heavy-mineral species are mainly subrounded, which suggests that the violation of the settling-equivalence principle is not caused by faster mechanical wear of clinopyroxene relative to tougher zircon in eolian environments.

The anomalous marked decrease in the ratio between ferromagnesian minerals and denser epidote with increasing grain size in the fine tail of the Taroot beach sample may reflect the finer size of detritus rich in amphibole and pyroxene largely derived from Anatolia via the Euphrates and Tigris Rivers than the less travelled epidote-rich detritus derived from the Zagros thrust belt exposed along the opposite side of the Gulf. The even more notably anomalous decrease in the amphibole/epidote ratio with grain size observed in the Tamani dune sample suggests mixing of amphibole-rich detritus carried by local widyan draining the Arabian shield with notably coarser detritus recycled from largely Paleozoic siliciclastic covers also supplying zircon, garnet, and staurolite.

Polymodal dune sands and the durability of sand grains

The markedly bimodal composition displayed by many coastal Jafurah (fig. 7 in Garzanti et al. 2013) and northeastern Rub' al Khali dunes (Fig. 4B,E) is largely ascribed to mixing of detrital populations with different provenance and grain size. Namely, the generally predominant coarser-grained sand derived from anorogenic Arabian covers, chiefly consisting of recycled monocrystalline quartz and a few feldspars (mainly K-feldspar), mixes with a subordinate to minor finer-grained lithic-rich population of orogenic provenance derived from Anatolia and the Zagros Mountains.

Other factors however, contribute to such notable intrasample compositional variability, including not only hydraulic sorting but also different resistance of different detrital minerals to mechanical abrasion. Greater toughness of chert relative to limestone grains (McBride and Picard 1987; Picard and McBride 2007) explains why the former - which are mainly subangular whereas the latter are almost invariably rounded to well rounded - increase relative to total sedimentary and metasedimentary lithics from 8±5% in the fine sand class to 28±12% in the medium sand class of dunes inland of Sabkha Matti (Fig. 7). Beside extensive recycling of rounded quartz grains (Fig. 5E), innumerable strong impacts in the eolian environment may represent an additional factor contributing to the dominance of rounded quartz in the coarse sand class (e.g., Fig. 4B). In southwestern Rub' al Khali dunes, the very small size of limestone grains (Fig. 5F) would indicate very limited resistance to mechanical wear if derived largely from nearby sources (e.g., Jabal Tuwaiq, Hadhramaut Arch), and may thus suggest long-distance transport all across the vast sand sea.

DETRITAL ZIRCON GEOCHRONOLOGY

In all 27 sand samples from Saudi Arabia detrital zircons yielded mostly Cambrian to Neoproterozoic ages (85±7% between 490 and 1100 Ma), reflecting crustal growth and amalgamation of the Arabian shield during the polyphase "Pan-African" orogenic events (Avigad et al. 2003; Johnson et al. 2011; Morag et al. 2011). Within such a broad, major "Pan-African" age cluster, U-Pb spectra show a major peak centered at 624 Ma, and subordinate ones at 750-820 Ma and 920-1030 Ma. Mid-Paleoproterozoic (1.74-2.15 Ga) and earliest Paleoproterozoic-Neoarchean clusters (2.40-2.73 Ga) occur in all samples but each represents < 5% of total grains in most. All detrital zircons are older than 350 Ma in sands of Wadi Dawasir, Hima, Hubuna and Najran, draining the Arabian shield and/or its Paleozoic covers, whereas minor populations of young zircons characterize Gulf beaches, Jafurah, and Rub' al Khali dunes (Fig. 8).

Grains with Miocene to Cretaceous ages represent between 1.8% and 3.7% of analysed zircons in Gulf beaches (five ages from 5 to 47 Ma and two at 70 and 96 Ma) and in eastern Jafurah (four from 26 to 46 Ma, seven from 74 to 113 Ma), inland Sabkha Matti (three from 34 to 50 Ma, seven from 71 to 100 Ma), Shaybah (six from 5 to 41 Ma, seven from 71 to 110 Ma), and Ardah dunes (two at 30 and 41 Ma, five from 77 to 99 Ma). Late-Middle Jurassic to Permian-Carboniferous zircons also occur, and form clusters in dunes inland of Sabkha Matti (five ages from 153 to 174 Ma, twelve from 260 to 333 Ma). Young grains are much rarer in southwestern Rub' al Khali dunes and sand sheets, where a few Devonian-Silurian ages were obtained but only four out of 1063 dated zircons yielded Cenozoic (47 Ma in the Sharurah dune), Mesozoic (98 and 244 Ma) or Upper Carboniferous ages (315 Ma).

SAND PROVENANCE FROM THE GULF TO THE NORTHEASTERN RUB' AL KHALI

Along the Arabian coast of the Gulf, intrabasinal allochems and extrasequential grains recycled from Pleistocene eolianites and underlying Miocene strata are mixed in various proportions with four different populations of extrabasinal terrigenous detritus (Fig. 10): 1) a quartzose population with a very poor heavy-mineral suite relatively rich in zircon, tourmaline and rutile ultimately derived from interior Arabia; 2) a feldspatho-quartzo-lithic population with a rich amphibole-pyroxene-epidote-garnet suite derived long-distance from Anatolia and the northern Zagros Mountains via the Euphrates and Tigris rivers; 3) a lithic carbonaticlastic population with a poor heavy-mineral suite relatively rich in epidote derived from the southern Zagros Mountains; 4) a lithic cherticlastic-carbonaticlastic to ultramaficlastic population with an up to very rich heavy-mineral suite characterized by enstatite derived from the Oman Mountains (Ahmed et al. 1998; Walkden and Williams 1998; El-Sayed 1999, 2000; Nasir et al. 1999). The detrital signatures of these four populations are defined in detail based on data also from Garzanti et al. (2002, 2003, 2013, 2016).

The mixing proportions of such four different detrital populations were quantified by forward mixing models based on integrated bulk-petrography and heavy-mineral data (Garzanti et al. 2012b; mathematical approach illustrated in Appendix A). Because we could not collect dune sand in the central part of the erg, two separate sets of calculations were performed for Gulf and northeastern Rub' al Khali sands (discussed in this section) and southwestern Rub' al Khali sands (presented in the next section below). For Gulf beaches and northeastern Rub' al Khali dunes, the four end-members were defined as the average composition of sands in: 1) Dahna dunes and Wadi Rimah-al Batin; 2) Euphrates and Tigris Rivers including sediments of the Mesopotamian floodplain; 3) Karun River and Shatt al Arab; 4) Oman pediment and widyan draining the southern flank of the northern Oman mountains. For southwestern Rub' al Khali dunes and sand sheets, three different Arabian end-members were defined as the average composition of sands in: 1a) Wadi Qatan and Wadi Hubuna for Arabian basement; 1b) Wadi Hima and Wajid sandstone for siliciclastic Paleozoic covers; 1c) Wadi Ushayrab and Wadi Maqran for mostly carbonate Mesozoic covers. Because recycling of Quaternary eolianites and underlying Miocene sandstones (Farrant et al. 2012) could not be quantified, all grains were considered as derived ultimately from source rocks. The effect of mechanical wear was neglected for the sake of simplicity, and contribution from carbonate-rich sources (e.g., Zagros fold-belt) may have thus been underestimated. Because of a far more accurate definition of Anatolia and Zagros end members, the estimates presented here are considered as better constrained than those obtained previously (Garzanti et al. 2003, 2013).

The recycled Arabian component

Because of scarce rainfall and modest relief, erosion rates and sediment yields are very low in the heart of the Arabian shield exposed along the gently tilted eastern flank of the Red Sea rift shoulder. As a consequence of low transport capacity, fluvial contribution to the sand seas is minor, as displayed by contrasting composition of wadi sand and adjacent eolian dunes at the edge of the ergs (figs. 5 and 6 in Garzanti et al. 2013). As soon as they leave the shield, even major widyan are rapidly choked by eolian sands largely generated by local disaggregation of siliciclastic cover strata. Extensive recycling of Paleozoic and subordinately Mesozoic units is indicated for the Great Nafud and Dahna dune fields of northern Arabia, containing virtually pure quartz sand with very poor heavy-mineral suites characterized by zircon, tourmaline and rutile (quartz 98±2% of bulk sediment, ZTR 45±11; Garzanti et al. 2013). Such a highly quartzose composition is never reached in dune sands of the western Jafurah (quartz 93.2±0.4%, ZTR 14±9) or northeastern Rub' al Khali dune fields (quartz 78±12%, ZTR 6±2), reflecting progressive mixing with low-quartz, low-ZTR orogenic detritus eastwards. Cambrian to Neoproterozoic U-Pb zircon ages are dominant in all of the studied samples, indicating that the majority of zircon grains in all Arabian dune fields as well as in beaches of the Gulf are ultimately derived from the Arabian basement assembled during multiphase "Pan African" orogenic events.

The orogenic Anatolia-Zagros component

Steady northward compositional changes of dune sand from the Uruq al Mutaridah to the Liwa oasis and the Trucial coast document mixing in increasing proportions with orogenic detritus derived long-distance from the Anatolia-Zagros orogen (figs. 4 and 8 in Garzanti et al. 2013). Orogenic contribution, documented by chert, volcanic, carbonate, low-rank metabasite and ultramafic grains, is estimated to increase progressively from 18±3% for feldspatho-quartzose sand in Ardah dunes, to 24±7% for feldspatho-quartzose sand in Shaybah dunes, 36±4% for litho-feldspatho-quartzose sand in Liwa dunes, 59±19% and 59±7% for feldspatho-litho-quartzose dune sand respectively inland of Sabkha Matti and in the intermediate belt of the UAE, and to 87±5% and 94±5% for quartzo-lithic sand respectively in dunes and beaches of the Trucial coast. The carbonaticlastic Zagros component, dominant in beaches and dunes of the Trucial coast, fades rapidly inland also partly because of selective mechanical wear of soft carbonate grains, and it is minor relative to the Mesopotamian (Tigris + Euphrates) component from the Liwa oasis to the Uruq al Mutaridah. Orogenic detritus, with prevalence of Mesopotamian over Zagros contribution, is estimated to increase eastward from 5±1% in quartzose sand of western Jafurah dunes to 35±10% in feldspatho-litho-quartzose to litho-fedlspatho-quartzose sand of coastal Jafurah and Niqyan Qatar dunes, and northward from only 4±3% in quartzose sand of Gulf beaches between Qatar and Dammam to 28±18% in quartzose to feldspatho-litho-quartzose sand between Dammam and Kuwait.

Because post-Devonian detrital zircons are absent in wadi sands derived from the Arabian shield and its siliciclastic cover units (Garzanti et al. 2013), young grains need to come from elsewhere. Miocene to Carboniferous zircons represent about a quarter of grains carried by the Euphrates (19%), Tigris (27%) and Karun Rivers (29%; Garzanti et al. 2016). Euphrates age-spectra are characterized by small Miocene-Oligocene (15-34 Ma) and Late Cretaceous clusters (77-98 Ma) with few Permian-Devonian grains, whereas Tigris spectra include small Eocene (33-57 Ma), mid-Late Cretaceous, (72-115 Ma), Middle Jurassic (167-169 Ma), Late Triassic (225-230 Ma) and Permian-Carboniferous clusters (285-338 Ma) with few Devonian-Silurian grains. The Karun carries to the Shatt al Arab a few zircons as young as 6-8 Ma and a continuum of Paleogene to Silurian zircons forming a major Jurassic (155-180 Ma) and a secondary Permian-Carboniferous cluster (290-315 Ma). Age clusters in the Euphrates-Tigris-Karun river system match well and thus explain the occurrence of small but significant Miocene-Eocene and mid-Late Cretaceous populations found in Gulf beaches and northeastern Rub' al Khali dunes (Fig. 8). Ages as young as latest Miocene in one beach and one dune sample, and Late-Middle Jurassic and Permian-Carboniferous clusters in dunes inland of Sabkha Matti are exclusive features of Karun sand, and thus point to ultimate Zagros provenance. Zircon-age fingerprints prove to represent a robust independent tool to trace detritus from the Anatolia-Zagros orogen into the northeastern Rub' al Khali Erg (Fig. 9).

The orogenic Oman component

The Rub' al Khali sand sea is delimited to the northeast by the Quaternary fanglomerate apron fed chiefly by Hawasina-type deep-water successions uplifted at the southern front of the northern Oman thrust belt (Maizels and McBean 1990; Blechschmidt et al. 2009). This gravelly pediment surface, formed by prolonged wind deflation that removed finer grains toward the Wahiba Sands, is mantled by small pebbles and granules of chert, with subordinate limestone, shale to sandstone, and minor volcanic and metavolcanic clasts (Fig. 4D). Dunes advancing on such substrate at the northeastern edge of the erg do contain locally slightly more abundant chert and enstatite grains, but their composition is altogether similar to Ardah dunes inland. Heavy-mineral concentration tends to decrease from Shaybah to Ardah, and ultramafic rock fragments remain rare, which rules out additional contribution from heavy-mineral-rich mafic and ultramafic rocks of the Sema'il ophiolite. Sediment supply from northern Oman ophiolites to Rub' al Khali dunes, overemphasized by previous authors (e.g., El-Sayed 1999, 2000), is in fact negligible even at the very edge of the sand sea (0.5±0.3% of bulk sand), and null in the Uruq al Mutaridah inland. Ophiolite-derived clasts increase in fanglomerates northward (Farrant et al. 2015), and yet detritus ultimately derived from the Oman obduction orogen reaches at most, and only locally close to the mountain front, 5-15% of feldspatho-litho-quartzose to feldspatho-quartzo-lithic sand of UAE dunes and beaches.

SAND PROVENANCE IN THE SOUTHWESTERN RUB' AL KHALI

Wadi sand in central to southern Saudi Arabia ranges from feldspatho-quartzose basementaclastic (Wadi Hubuna and Qatan) to recycled quartzose (Wadi Hima) and quartzo-lithic carbonaticlastic (Wadi Hanifa/Sahba, Ushayrab, Maqran, and Sulayyil), reflecting provenance from the Arabian shield and its Paleozoic to Jurassic sedimentary covers in different proportions. Sand of Wadi ad Dawasir is a mixture of detritus derived from crystalline basement, siliciclastic and carbonate cover strata diluted by finer-grained wind-blown quartz. Sand of Wadi Najran is largely recycled from Paleozoic siliciclastic covers.

Detrital signatures of wadi sands are much more varied than those of sand sheets and dunes in the adjacent sand sea, characterized by dominant quartz and poor heavy-mineral suites with zircon, tourmaline and rutile. Such a concentration of chemically durable minerals reflects extensive recycling of mostly Paleozoic siliciclastic units, and is thus inherited chiefly from the Cambro-Ordovician period of intense weathering that followed the end of the Neoproterozoic orogeny (Avigad et al. 2005). Most dunes, however, are not as quartzose as the Wajid Sandstone, and heavy-mineral concentration is one to two orders-of-magnitude higher with much lower ZTR indices (7±4 vs. 54). This indicates an additional contribution from the Arabian shield, estimated to account for ~20% of dune sand. Moreover, only the coarse tail of the size distribution is invariably quartzose to purely quartzose, whereas the fine tail may contain significant feldspar, carbonate and diverse other lithic grains. Heavy-mineral concentration, highest in sand sheets and low dunes along the western edge of the desert where amphibole is most abundant, tends to decrease toward the heart of the sand sea (corr. coeff. ~0.8, sign. lev. 0.1%), where suites become progressively closer to those in the northeastern Rub' al Khali. Some similarities in petrographic and heavy-mineral modes between the southwestern and northeastern Rub' al Khali may suggest homogenization at the regional scale within the sand sea. Detrital modes, however, do not indicate extensive mixing with orogenic detritus transported all across the erg. The few small carbonate grains found in southwestern Rub' al Khali dunes may be blown by dominant Shamal winds from as far as the Gulf and beyond, but also derived locally from carbonate outcrops of Jabal Tuwaiq and the Hadhramaut Arch or supplied by Wadi ad Dawasir. Also the few sedimentary/metasedimentary, metavolcanic/metabasite and chert grains, equally concentrated in the fine tail of the size distribution (Fig. 6A,B), may be derived either locally from the Arabian basement and cover strata or long-distance ultimately from as far as the Anatolia-Zagros orogen. Detrital zircons mostly yielded Early Paleozoic and Precambrian ages, indicating overwhelming supply from Arabian sources. The rare occurrence of zircon grains yielding Eocene to Carboniferous ages, however, suggests that Arabian detritus may not be exclusive even along the southwestern edge of the Rub' al Khali. The possibility of eolian transport by Shamal winds for ~1000 km across the sand sea, and ultimate provenance of a minor part of dune sand from as far as the Anatolia-Zagros orogen cannot be ruled out.

CONCLUSIONS

By using petrographic, heavy-mineral and geochronological signatures of sand-sized grains we have documented an exceptional case of transcontinental multi-step sediment transport in hyperarid climatic conditions along a particularly complex routing system (Fig. 11). Detritus shed by the Anatolia-Zagros orogen developed on the Eurasian upper plate after collision with Arabia in the Paleogene did not only reach the associated Gulf foreland basin on the lower plate via the Euphrates-Tigris system and other rivers draining the Iranian Zagros, but it was blown inland by dominant Shamal winds to reach well into the Arabian foreland. Sediment dispersal over a cumulative distance of up to 4000 km from Anatolian headwaters took place in multiple steps through the Quaternary, involving repeated eolian reworking of Quaternary and Neogene foreland-basin deposits during lowstand stages of the Pleistocene and progressive accumulation of dunes in the Rub' al Khali, the largest continuous sand sea on Earth.

The extrabasinal sand fraction in Gulf beaches and northeastern Rub' al Khali dunes is ultimately derived from Arabia, Anatolia, and the Zagros in varying proportions. Sediment supply from obducted ophiolites of the northern Oman Mountains is instead detected only locally, and largely negligible overall. Sand of the southwestern Rub' al Khali is dominantly Arabian-derived, but similarities of compositional parameters and a few young zircon ages suggest the possibility of long-distance mixing with sand blown all the way from the Gulf coast to as far as the southwestern edge of the sand sea. Besides the progressive dilution inland by coarser quartzose sand mostly recycled from Arabian siliciclastic covers, mechanical wear during long-distance transport in high-energy eolian environments explains why relatively soft carbonate grains are systematically concentrated in the finer sand class, as observed in beaches and dunes along the Gulf coast and in the northeastern to southwestern Rub' al Khali. The complexity of sediment dispersal patterns, commonly extending across a continent over distances of thousands of kilometers, and the consequent spatial decoupling between diverse detrital sources and the depositional sink must be carefully taken into account when interpreting provenance and dispersal pathways of ancient clastic suites.

ACKNOWLEDGMENTS

Petrographic analyses on several samples were carried out by Danilo Controversio; Stefano Lombardi helped with heavy-mineral analyses and George Peters with U-Pb geochronological analyses. Luca Caracciolo kindly collected the Kuwait beach sand. Information and advice from Kenneth Glennie and assistance in the field by Abduljamiu Olalekan Amao and Ardiansyah Koeshidayatullah is gratefully acknowledged. The article benefited greatly from extremely careful, excellent constructive comments by reviewers Bill Heins and Tim Lawton and editors Lynn Soreghan and Gary Hampson.

SUPPLEMENTARY MATERIAL

Supplementary data associated with this article can be found in the online version, at http://dx.doi.___________. These include information on sampling sites (Table A1) and the complete bulk-sand petrography (Table A2), heavy-mineral (Table A3), and geochronological datasets (Appendix B). Table captions are contained in Appendix A, which illustrates the approach followed in the calculation of provenance budgets. The Google Earth™ map of sampling sites *Arabia&Gulf.kmz* is also provided.

FIGURES

Figure 1. Google Earth™ map of Arabia and the Anatolia-Zagros orogen showing sample locations. The Euphrates-Tigris-Karun drainage basin is outlined by thick grey line. Thin orange lines indicate dune trends in the Rub' al Khali Erg; thickness of blue lines is proportional to the importance of each river/wadi. The two white dotted arrows indicate traverses across the northwestern and northeastern edges of the Rub' al Khali illustrated by microphotographs *A-B-C* and *D-E-F* in Figure 4. Samples labeled with small-case letters around the southwestern edge of the Rub' al Khali refer to microphotographs *a-b-c-d-e-f* in Figure 5.

Figure 2. Geology of Arabia and the Gulf region (redrawn from Asga-Unesco 1963), where sand seas occupy an area of ~800,000 km^2 overall.

Figure 3. Geography of Arabia and the Gulf region. Modern seasonal wind regimes after the *Saudi Arabian Wind Energy Atlas* cited in Al-Ali (2015).

Figure 4. Petrographic trends along two traverses at the northwestern and northeastern edges of the Rub' al Khali (sample location shown in Fig. 1). **Northwestern traverse**: **A**) feldspatho-litho-quartzose Gulf beach sand of largely Anatolia-Zagros provenance; **B**) bimodal dune sand including Arabian-derived quartz associated with a much finer-grained feldspatho-litho-quartzose carbonaticlastic fraction of largely Anatolia-Zagros provenance; **C**) feldspatho-quartzose dune sand farther inland lacking carbonate grains. **Northeastern traverse**: **D**) cherticlastic gravel pediment fed mostly from the Hawasina Nappes of the northern Oman Mountains; **E**) dune sand containing abundant tiny carbonate grains; **F**) feldspatho-quartzose dune sand farther inland lacking carbonate grains. Q = quartz; K = K-feldspar; P = plagioclase; rock fragments: C = carbonate, H = chert, A = arenaceous, V = volcanic; p = pyroxene. Blue bar for scale = 250 µm.

Figure 5. Petrographic signatures and sand sources in the southwestern Rub' al Khali. **A**) Carbonaticlastic wadi sand from Jurassic strata of Jabal Tuwaiq. **B**) Mixed basementaclastic and sedimentaclastic wadi sand from the Arabian shield and its cover strata. **C**) Basementaclastic wadi sand from the Arabian shield. **D**) Highly quartzose sand recycled from Paleozoic sandstones. **E**) Paleozoic quartzose sandstone. **F**) Bimodal feldspatho-quartzose dune sand with a very-fine-grained population containing abundant carbonate grains. Q = quartz; K = K-feldspar; P = plagioclase; C = carbonate rock fragments. Blue bar for scale = 250 μm.

Figure 6. Intrasample compositional variability (analytical data provided at bottom of Appendix Tables A2 and A3; petrographic parameters as in Table 1 and Fig. 10). In the QFL plot **A**, data are centered to allow better visualization (von Eynatten et al. 2002; Comas-Cufí and Thió-Henestrosa 2011). In the compositional biplots **B** and **C**, both multivariate observations (points) and variables (rays) are displayed (Gabriel 1971). The length of each ray is proportional to the variability of the parameter in the data set. If the angle between two rays is close to 0°, 90°, and 180°, then the corresponding parameters are directly correlated, uncorrelated, and inversely correlated, respectively. **A**, **B**) Provenance-controlled intrasample variability of petrographic modes is regulated principally by increasing proportions of Arabian-derived quartzose detritus with grain size relatively to either finer-grained lithic-rich sedimentaclastic orogenic detritus in dunes inland of Sabkha Matti or feldspar-bearing detritus derived from the Arabian shield in southwestern Rub' al Khali dunes. Orogenic detritus fades landward of Shaybah and Ardah, where intrasample compositional variability is less marked. The southernmost Rub' al Khali Sharurah dune shows similar variability pattern as dunes inland of Sabkha Matti, owing to either local addition of mainly sedimentary lithic grains from the Hadhramaut arch or possibly to mixing with eolian sand blown long-distance from the Gulf. **C**) Intrasample variability of heavy-mineral modes is primarily a settling-equivalence effect (denser minerals concentrate progressively in finer classes) superposed

on provenance effects. Gulf beaches are richer in clinopyroxene and garnet, southwestern Rub' al Khali dunes in amphibole and zircon. The anomalous correlation patterns with heavy-mineral concentration (low-density tourmaline is inversely correlated as expected, but epidote and garnet should correlate better than less dense amphibole and clinopyroxene) indicates mixing with finer-grained detritus enriched in ferromagnesian minerals.

Figure 7. Influence of mechanical wear on downwind compositional changes (data are centered to allow better visualization). Because of mixing with quartz-rich Arabian-derived sand, sedimentary lithics decrease progressively inland from the Gulf to the northeastern Rub' al Khali, but carbonate (Lc) and shale/siltstone grains (Lp) decrease notably faster than tougher chert (Lh). Chert increases from finer to coarser sand classes within dunes inland of Sabkha Matti, which also suggests greater resistance to mechanical wear. Only a little chert from the Oman Mountains is added locally at the eastern edge of the erg; Arabian sources at its western edge may contribute carbonate lithics but no chert.

Figure 8. U-Pb age spectra of detrital zircons (age vs. frequencies plotted as Kernel Density Estimates using the *provenance* package of Vermeesch et al. 2016). Arabian sources are dominated by Cambrian to Neoproterozoic "Pan-African" zircons and lack post-Devonian zircons, which are common in Euphrates-Tigris-Karun sands. A few zircons as young as the latest Miocene as well as small Oligocene-Eocene, Late Cretaceous, Middle Jurassic, and Permian-Carboniferous clusters found from Gulf beaches to northeastern Rub' al Khali dunes allow us to trace orogenic detritus ultimately derived from the Anatolia-Zagros orogen into the heart of Arabia.

Figure 9. Multidimensional scaling map of Arabian sands based on U-Pb ages of detrital zircons (plotted using the *provenance* package of Vermeesch et al. 2016). The distance among samples is approximately proportional to the Kolmogorov-Smirnov dissimilarity of their zircon-age spectra;

the 'stress' value of the configuration is 5.9%, indicating a 'good' fit (Vermeesch 2013). The two main ultimate sources of detrital zircons are the Tigris-Euphrates-Karun fluvial system in the north and Arabia with its siliciclastic covers in the west. Zircon grains mix progressively during sand dispersal from north to south to finally reach the Rub’ al Khali Erg. Data from northern Arabian deserts, Paleozoic sandstones and the Euphrates-Tigris-Karun river system after Garzanti et al. (2013; 2016).

Figure 10. Provenance analysis. Beaches of the northern Gulf and dunes from the Jafurah to the northeastern Rub' al Khali ergs are derived partly from Mesopotamian sources (Euphrates + Tigris Rivers), with contribution from Arabian sources (mostly Paleozoic siliciclastic strata) rapidly increasing landward and with increasing grain size. Composition of Trucial coast beaches and dunes points to major ultimate supply from the Zagros Mountains along the opposite side of the Gulf (Garzanti et al. 2003). Dunes of the southwestern Rub' al Khali are chiefly Arabian-derived. **A**) QFL plot (data are centered to allow better visualization). Feldspatho-quartzo-lithic Mesopotamian sands carried by the Euphrates and Tigris Rivers and lithic carbonaticlastic Zagros sands supplied by the Karun and Shatt al Arab are sharply distinct from feldspatho-quartzose and quartzose sands derived from the Arabian shield and its Paleozoic siliciclastic covers. Mainly quartzo-lithic carbonaticlastic detritus shed by Arabian Mesozoic covers contributes little to the dune fields. **B**) Framework petrography. **C**) Heavy minerals. Intrasample variability follows the settling-equivalence-controlled pattern towards decreasing heavy-mineral concentration with increasing grain size in both Taroot beach and Tamani dune samples, but also shows a prominent provenance effect for the Taroot beach, composition moving away from the Mesopotamian field towards the Arabian field with increasing grain size (arrow). **D**) Petrographic and heavy-mineral signatures combined. L= lithic grains (Lvm = volcanic and low-rank metavolcanic; Lsm = sedimentary and low-rank metasedimentary; Lmfb = high-rank felsic metamorphic and metabasite); op= opaque Fe-Ti-Cr oxides; other parameters as in Table 1.

Figure 11. The complex source-to-sink system of Arabian sands. The twelve mineralogical maps illustrate key petrographic and heavy-mineral data; circles stand for sample groups, with diameter proportional to size of source or sink, color fill proportional to mineral abundance, and color outline representing facies (green = river/wadi; blue = beach; orange = eolian dune/sand sheet; purple = pediment). Reconstructed in the central panel are patterns of sand dispersal and mixing (arrow thickness indicatively proportional to estimated contribution). Only ultimate sources of detritus are shown, because our data cannot reveal multiple recycling of Pleistocene eolianites and Miocene sandstones. Sand contributions from Anatolia, Zagros Mountains, Arabian Shield, Sama'il ophiolite, or even from Hawasina cherts and local outcrops of carbonate rocks or Neogene basalts are identified more readily at the periphery of sand seas, whereas monocrystalline quartz becomes rapidly dominant toward the core of all major Arabian ergs. Quartz recycled from Paleozoic or younger siliciclastic strata thus represents by far the dominant source of sand to Arabian deserts, reflecting the high sand-generation potential of quartz-rich sandstones.

Table 1. Key petrographic and mineralogical parameters of sands from Mesopotamian rivers, Gulf beaches, and Arabian dune fields and widyan (Fig. 1; including data from Garzanti et al. 2001, 2003, 2013, 2016) . N°= number of samples; Q= quartz; F= feldspars (KF= K-feldspar; P= plagioclase); L= lithic grains (Lc= carbonate; Lh= chert; Lms= other sedimentary and metasedimentary; Lmv = volcanic, metavolcanic, and metabasite; Lu= ultramafic). HM= heavy minerals. tHMC = transparent Heavy-Mineral Concentration. ZTR = zircon + tourmaline + rutile; Ep = epidote; Grt = garnet; CSKA = chloritoid + staurolite + andalusite + kyanite + sillimanite; Amp = amphibole; Cpx = clinopyroxene; En= enstatite; Hy= hypersthene; Ol = olivine; Sp = Cr-spinel; &tHM = other transparent heavy minerals (titanite, apatite, minor Ti oxides and monazite). Full datasets provided in Appendix Tables A2 and A3.

REFERENCES

Ahmed, E.A., Soliman, M.A., Alsharhan, A.S., and Tamer, S., 1998, Mineralogical characteristics of the dunes in the Eastern Province of Abu Dhabi, United Arab Emirates, *in* Alsharhan, A.S., Glennie, K.W., Whittle, G.L., and Kendall, C.G.St.C., eds., Quaternary Deserts and Climatic Change: Rotterdam, Balkema, p. 85-90.

Al-Ajmi, H.F., Keller, M., Hinderer, M., and Filomena, C.M., 2015, Lithofacies, depositional environments and stratigraphic architecture of the Wajid Group outcrops in southern Saudi Arabia: GeoArabia, v. 20, p. 49-94.

Al-Ali, A.M., 2015, Use of spatial technologies to study the winds' directions in Rub' Al-Khali Desert, Saudi Arabia: Journal of Earth Science and Engineering, v. 5, p. 372-381.

Al-Saad, H., Nasir, S., Sadooni, F., and Alsharhan A.S., 2002, Stratigraphy and sedimentology of the Hofuf Formation in the State of Qatar in relation to the tectonic evolution of the East Arabian Block: Neues Jahrbuch für Geologie und Paläontologie-Monatshefte, v. 7, p. 426-448.

Alsharhan, A.S., and Kendall, C.G.St.C., 2003, Holocene coastal carbonates and evaporites of the southern Arabian Gulf and their ancient analogues: Earth-Science Reviews, v. 61, p. 191-243.

Alsharhan, A.S., and Nairn, A.E.M., 1997, Sedimentary basins and petroleum geology of the Middle East: Amsterdam, Elsevier, 942 p.

Al-Sulaimi, J.S., and Pitty, A.F., 1995, Origin and depositional model of Wadi Al-Batin and its associated alluvial fan, Saudi Arabia and Kuwait: Sedimentary Geology, v. 97, p. 203-229.

Andò, S., and Garzanti, E., 2014, Raman spectroscopy in heavy-mineral studies: Geological Society London, Special Publication 386, p. 395-412.

Anton, D., 1983, Modern eolian deposits of the eastern province of Saudi Arabia, *in* Brookfield, M.E., and Ahlbrandt, T.S., eds., Eolian sediments and processes: Amsterdam, Elsevier, Developments in Sedimentology, v. 38, p. 365-378.

Asga-Unesco, 1963, Geological map of Africa, sheet N.3, scale 1:5,000,000: Association of African Geological Surveys, United Nations Educational, Scientific and Cultural Organization, Paris.

Avigad, D., Kolodner, K., McWilliams, M.O., Persing, H.M., and Weissbrod, T., 2003, Origin of northern Gondwana Cambrian sandstone as revealed by SHRIMP dating of detrital zircons: Geology, v. 31, p. 227-230.

Avigad, D., Sandler, A., Kolodner, K., Stern, R.J., McWilliams, M.O., Miller, N., and Beyth, M., 2005, Mass-production of Cambro-Ordovician quartz-rich sandstone as a consequence of chemical weathering of Pan-African terranes: environmental implications: Earth and Planetary Science Letters, v. 240, p. 818-826.

Baltzer, F., and Purser, B.H., 1990, Modern alluvial fan and deltaic sedimentation in a foreland tectonic setting: the lower Mesopotamian plain and the Arabian Gulf: Sedimentary Geology, v. 67, p. 175-197.

Béchennec, F., Le Métour, J., Rabu, D., Bourdillon-De-Grissac, C., De Wever, P., Beurrier, M., and Villey, M., 1990, The Hawasina Nappes: stratigraphy, palaeogeography and structural evolution of a fragment of the south-Tethyan passive continental margin: Geological Society London, Special Publication 49, p. 213-223.

Bibi, F., Hill, A., Beech, M., and Yasin, W., 2013, Late Miocene fossils from the Baynunah Formation, United Arab Emirates: summary of a decade of new work, *in* Wang, X., Flynn, L.J., and Fortelius, M., eds., Fossil mammals of Asia: Neogene biostratigraphy and chronology, p. 583-594.

Bishop, M.A., 2013, Dune field development, interactions and boundary conditions for crescentic and stellate megadunes of the Al Liwa Basin, the Empty Quarter: Earth Surface Processes and Landforms, v. 38, p. 183-191.

Blechschmidt, I., Matter, A., Preusser, F., and Rieke-Zapp, D., 2009, Monsoon triggered formation of Quaternary alluvial megafans in the interior of Oman: Geomorphology, v. 110, p. 128-139.

Cantrell, D. L., Nicholson, P.G., Hughes, G.W., Miller, M.A., Bhullar, A.G., Abdelbagi, S.T., and Norton, A.K., 2014, Tethyan petroleum systems of Saudi Arabia: American Association of Petroleum Geologists, Memoir 106, p. 613-639.

Comas-Cufí, M., and Thió-Henestrosa, S., 2011, CoDaPack 2.0: a stand-alone, multiplatform compositional software. In: CoDaWork'11: 4th International Workshop on Compositional Data Analysis. Sant Feliu de Guíxols, Spain.

Dickinson, W.R., 1988, Provenance and sediment dispersal in relation to paleotectonics and paleogeography of sedimentary basins, *in* Kleinspehn, K.L., and Paola, C., eds., New perspectives in basin analysis: New York, Springer, p. 3-25.

Edgell, H.S., 2006, Arabian deserts: nature, origin and evolution: Dordrecht, Springer, 591 p.

El-Sayed, M.I., 1999, Sedimentological characteristics and morphology of the aeolian sand dunes in the eastern part of the U.A.E.: a case study from Ar Rub' Al Khali: Sedimentary Geology, v. 123, p. 219-238.

El-Sayed, M.I., 2000, The nature and possible origin of mega-dunes in Liwa, Ar Rub' Al Khali, U.A.E.: Sedimentary Geology, v. 134, p. 305-330.

Evans, G., 2011, An historical review of the Quaternary sedimentology of the Gulf (Arabian/Persian Gulf) and its geological impact, *in* Kendall, C.G.St, and Alsharhan, A., eds., Quaternary carbonate and evaporite sedimentary facies and their ancient analogues: a tribute to D.J. Shearman: Chichester, Wiley-Blackwell, International Association of Sedimentologists, Special Pubblication 43, p. 11-44.

Farrant, A.R., Ellison, R.A., Thomas, R.J., Pharaoh, T.C., Newell, A.J., Goodenough, K.M., Lee, J.R., and Knox, R.O.B., 2012, The Geology and Geophysics of the United Arab Emirates. Volume 6: Geology of the western and central United Arab Emirates: British Geological Survey, v. 6, Keyworth, Nottingham.

Farrant, A.R., Duller, G.A., Parker, A.G., Roberts, H.M., Parton, A., Knox, R.W., and Bide, T., 2015, Developing a framework of Quaternary dune accumulation in the northern Rub'al-Khali, Arabia: Quaternary International, v. 382, p. 132-144.

Friend, P.F., 1999. Rivers of the Lower Baynunah Formation, Emirate of Abu Dhabi, United Arab Emirates. Fossil vertebrates of Arabia, with emphasis on the Late Miocene faunas, geology, and palaeoenvironments of the Emirate of Abu Dhabi, United Arab Emirates: New Haven, Yale University Press, p. 39-49.

Fryberger, S.G., Al-Sari, A.M., and Clisham, T.J., 1983, Eolian dune, interdune, sand sheet, and siliciclastic sabkha sediments of an offshore prograding sand sea, Dhahran area, Saudi Arabia: American Association of Petroleum Geologists Bulletin, v. 67, p. 280-312.

Fryberger, S.G., Al-Sari, A.M., Clisham, T.J., Rizvi, S.A.R., and Al-Hinai, K.G., 1984, Wind sedimentation in the Jafurah sand sea, Saudi Arabia: Sedimentology, v. 31, p. 413–431.

Gabriel, K.R., 1971, The biplot graphic display of matrices with application to principal component analysis: Biometrika, v. 58, p. 453-467.

Galehouse, J.S., 1971, Point counting, *in* Carver, R.E., ed., Procedures in sedimentary petrology: New York, Wiley, p. 385-407.

Garzanti, E., 1991, Non-carbonate intrabasinal grains in arenites: their recognition, significance and relationship to eustatic cycles and tectonic setting: Journal of Sedimentary Petrology, v. 61, p. 959-975.

Garzanti, E., 2016, From static to dynamic provenance analysis - Sedimentary petrology upgraded: Sedimentary Geology, v. 336, p. 3-13.

Garzanti E., 2017, The maturity myth in sedimentology and provenance analysis: Journal of Sedimentary Research, v. 87, p. 353-365.

Garzanti, E., and Andó, S., 2007, Heavy-mineral concentration in modern sands: implications for provenance interpretation, *in* Mange, M.A., and Wright, D.T., eds., Heavy Minerals in Use: Amsterdam, Elsevier, Developments in Sedimentology, v. 58, p. 517-545.

Garzanti, E., and Vezzoli, G., 2003, A classification of metamorphic grains in sands based on their composition and grade: Journal of Sedimentary Research, v. 73, p. 830-837.

Garzanti, E., Vezzoli, G., Andò, S., and Castiglioni, G., 2001, Petrology of rifted-margin sand (Red Sea and Gulf of Aden, Yemen): The Journal of Geology, v. 109, p. 277-297.

Garzanti, E., Vezzoli, G., and Andò, S., 2002, Modern sand from obducted ophiolite belts (Oman, U.A.E.): The Journal of Geology, v. 110, p. 371-391.

Garzanti, E., Andó, S., Vezzoli, G., and Dell'Era, D., 2003, From rifted margins to foreland basins: investigating provenance and sediment dispersal across desert Arabia (Oman, UAE): Journal of Sedimentary Research, v. 73, p. 572-588.

Garzanti E., Andò S., and Vezzoli G., 2008, Settling equivalence of detrital minerals and grain-size dependence of sediment composition: Earth and Planetary Science Letters, v. 273, p. 138-151.

Garzanti, E., Andò, S., Vezzoli, G., Lustrino, M., Boni, M., and Vermeesch, P., 2012a, Petrology of the Namib sand sea: long-distance transport and compositional variability in the wind-displaced Orange Delta: Earth-Science Reviews, v. 112, p. 173-189.

Garzanti, E., Resentini, A., Vezzoli, G., Andó, S., Malusà, M., and Padoan, M., 2012b, Forward compositional modelling of alpine orogenic sediments: Sedimentary Geology, v. 280, p. 149-164.

Garzanti, E., Vermeesch, P., Andó, S., Vezzoli, G., Valagussa, M., Allen, K., Khadi, K.A., and Al-Juboury, I.A., 2013, Provenance and recycling of Arabian desert sand: Earth-Science Reviews, v. 120, p. 1-19.

Garzanti, E., Vermeesch, P., Andò, S., Lustrino, M., Padoan, M., and Vezzoli, G., 2014, Ultra-long distance littoral transport of Orange sand and provenance of the Skeleton Coast Erg (Namibia): Marine Geology, v. 357, p. 25-36.

Garzanti, E., Andó, S., Padoan, M., Vezzoli, G., and El Kammar, A., 2015, The modern Nile sediment system: processes and products: Quaternary Science Reviews, v. 130, p. 9-56.

Garzanti, E., Al-Juboury, A.I., Zoleikhaei, Y., Vermeesch, P., Jotheri, J., Akkoca, D.B., Obaid, A.K., Allen, M.B., Andò, S., Limonta, M., Padoan, M., Resentini, A., Rittner, M., and Vezzoli, G., 2016, The Euphrates-Tigris-Karun river system: provenance, recycling and dispersal of quartz-poor foreland-basin sediments in arid climate: Earth-Science Reviews, v. 162, p. 107-128.

Glennie, K.W., 1998, The desert of southeast Arabia: a product of Quaternary climatic change, *in* Alsharhan, A.S., Glennie, K.W., Whittle, G.L., and Kendall, C.G.St.C., eds., Quaternary Deserts and Climatic Change: Rotterdam, Balkema, p. 279-291.

Glennie, K.W., and Singhvi, A.K., 2002, Event stratigraphy, paleoenvironment and chronology of SE Arabian deserts: Quaternary Science Reviews, v. 21, p. 853-869.

Glennie, K.W., Boeuf, M.G.A., Hughes-Clarke, M.W., Moody-Stuart, M., Pilar, W.F.H., and Reinhardt, B.M., 1974, Geology of the Oman Mountains: The Hague, Verhandelingen van het Koninklijk Nederlands Geologisch Mijnbouwkundig Genootschap, Transactions 31, 423 p.

Goudie, A.S., Colls, A., Stokes, S., Parker, A., White, K., and Al-Farraj, A., 2000, Latest Pleistocene and Holocene dune construction at the north-eastern edge of the Rub Al Khali, United Arab Emirates: Sedimentology, v. 47, p. 1011-1021.

Griffin, W.L., Powell, W.J., Pearson, N.J., and O'Reilly, S.Y., 2008, GLITTER: data reduction software for laser ablation ICP–MS, *in* Sylvester, P., ed., Laser ablation–ICP–MS in the earth sciences: current practices and outstanding issues: Mineralogical Association of Canada, Short Course 40, p. 204-207.

Hadley, D.G., Brouwers, E.M., Bown, T.M., 1998. Quaternary paleodunes, Arabian Gulf coast, Abu Dhabi Emirate: age and paleoenvironmental evolution. In: Alsharhan, A.S., Glennie, K.W., Whittle, G.L., Kendall, C.G.St.C. (Eds.), Quaternary Deserts and Climatic Change. Balkema, Rotterdam, pp. 123-139.

Harrell, J., and Blatt, H., 1978, Polycrystallinity: effect on the durability of detrital quartz: Journal of Sedimentary Petrology, v. 48, p. 25-30.

Hill, A., Bibi, F., Beech, M., and Al Tikriti, W.Y., 2012, Before archaeology: life and environments in the Miocene of Abu Dhabi, *in* Potts, D., Hellyer, P., eds., Fifty years of Emirates archaeology: Abu Dhabi, Ministry of Culture, Youth and Community Development, p. 20-33.

Holm, D.A., 1960, Desert geomorphology of the Arabian Peninsula: Science, v. 132, p. 1369-1379.

Hubert, J.F., 1962, A zircon-tourmaline-rutile maturity index and the interdependence of the composition of heavy mineral assemblages with the gross composition and texture of sandstones: Journal of Sedimentary Petrology, v. 32, p. 440-450.

Ingersoll, R.V., Bullard, T.F., Ford, R.L., Grimm, J.P., Pickle, J.D., and Sares, S.W., 1984, The effect of grain size on detrital modes: a test of the Gazzi–Dickinson point-counting method: Journal of Sedimentary Petrology, v. 54, p. 103-116.

Ingersoll, R.V., Dickinson, W.R., and Graham, S.A., 2003, Remnant-ocean submarine fans: largest sedimentary systems on Earth, *in* Chan, M.A., and Archer, A.W., eds., Extreme depositional environments: mega end members in geologic time: Geological Society of America, Special Paper 370, p.191-208.

Johnson, P.R., Andresen, A., Collins, A.S., Fowler, A.R., Fritz, H., Ghebreab, W., Kusky, T., and Stern, R.J., 2011, Late Cryogenian–Ediacaran history of the Arabian–Nubian Shield: a review of depositional, plutonic, structural, and tectonic events in the closing stages of the northern East African Orogen: Journal of African Earth Sciences, v. 61, p. 167-232.

Kendall, C.G.St, and Alsharhan, A., 2011, Quaternary carbonate and evaporite sedimentary facies and their ancient analogues: a tribute to D.J. Shearman: Chichester, Wiley-Blackwell, International Association of Sedimentologists, Special Pubblication 43, 496 p.

Lambeck, K., 1996, Shoreline reconstructions for the Persian Gulf since the last glacial maximum: Earth and Planetary Science Letters, v. 142, p. 43-57.

Limonta, M., Garzanti, E., Resentini, A., Andó, S., Boni, M., and Bechstädt, T., 2015, Multicyclic sediment transfer along and across convergent plate boundaries (Barbados, Lesser Antilles): Basin Research, v. 27, p. 696-713.

Lippard, S.J., Shelton, A.W., and Gass, I.G., 1986, The ophiolites of northern Oman: London, Blackwell, 178 p.

Lomando, A.J., 1999, Structural influences on facies trends of carbonate inner ramp systems, examples from Kuwait-Saudi Arabian coast of the Arabian Gulf and northern Yucatan, Mexico: GeoArabia, v. 4, p. 339-360.

Maizels, J., and McBean, C., 1990, Cenozoic alluvial fan systems of interior Oman: palaeoenvironmental reconstruction based on discrimination of palaeochannels using remotely sensed data: Geological Society London, Special Publication 49, p. 565-582.

McBride, E.F., and Picard, D.M., 1987, Downstream changes in sand composition, roundness and gravel size in a short-headed, high-gradient stream, Northwestern Italy: Journal of Sedimentary Petrology, v. 57, p. 1018-1026.

McClure, H.A., 1984, Late Quaternary palaeoenvironments of the Rub' Al Khali: University of London, Ph.D. Thesis, 245 p.

Morag, N., Avigad, D., Gerdes, A., Belousova, E., and Harlavan, Y., 2011, Crustal evolution and recycling in the northern Arabian–Nubian Shield: new perspectives from zircon Lu–Hf and U–Pb systematics: Precambrian Research, v. 186, p. 101-116.

Nasir, S.J., El-Kassas, I.A., and Sadiq, A.A.M., 1999, Mineralogy and genesis of heavy minerals in coastal dune sands, south eastern Qatar: Qatar University Science Journal, v. 19, p. 184-201.

Picard, M.D., and McBride, E.F., 2007, Comparison of river and beach sand composition with source rocks, Dolomite Alps drainage basins, northeastern Italy: Geological Society of America, Special Paper 420, p. 1-12.

Pugh, J.M., 1997, The Quaternary desert sediments of the Al Liwa area, Abu Dhabi: University of Aberdeen, Ph.D. Thesis, 316 p.

Purser, B.H., 1973, The Persian Gulf; Holocene carbonate sedimentation and diagenesis in a shallow epicontinental sea: New York, Springer, 471 p.

Radies, D., Preusser, F., Matter, A., and Mange, M., 2004, Eustatic and climatic controls on the sedimentary architecture of the Wahiba Sand Sea, Sultanate of Oman: Sedimentology, v. 51, p. 1359-1385.

Rittner, M., Vermeesch, P., Carter, A., Bird, A., Stevens, T., Garzanti, E., Andò, S., Vezzoli, G., Dutt, R., Xu, Z., and Lu, H., 2016, The provenance of Taklamakan desert sand. Earth and Planetary Science Letters, v. 437, p.127-137.

Rubey, W.W., 1933, The size-distribution of heavy minerals within a water-laid sandstone: Journal of Sedimentary Petrology, v. 3, p. 3-29.

Searle, M.P., James, N.P., Calon, T.J., and Smewing, J.D., 1983, Sedimentological and structural evolution of the Arabian continental margin in the Musandam Mountains and Dibba zone, United Arab Emirates: Geological Society of America Bulletin, v. 94, p. 1381-1400.

Stokes, S., and Bray, H.E., 2005, Late Pleistocene eolian history of the Liwa region, Arabian Peninsula: Geological Society of America Bulletin, v. 117, p. 1466-1480.

Teller, J.T., Glennie, K.W., Lancaster, N., and Singhvi, A.K., 2000, Calcareous dunes of the United Arab Emirates and Noah's flood: the postglacial reflooding of the Persian (Arabian) Gulf: Quaternary International, v. 68, p. 297-308.

Uchupi, E., Swift, S.A., and Ross, D.A., 1999, Late Quaternary stratigraphy, paleoclimate and neotectonism of the Persian (Arabian) Gulf region: Marine Geology, v. 160, p. 1-23.

Vermeesch, P., 2012, On the visualisation of detrital age distributions: Chemical Geology, v. 312-313, p. 190-194.

Vermeesch, P., 2013, Multi-sample comparison of detrital age distributions: Chemical Geology, v. 341, p. 140-146.

Vermeesch, P., Resentini, A., and Garzanti, E., 2016, An R package for statistical provenance analysis: Sedimentary Geology, v. 336, p. 14-25.

Vermeesch, P., Rittner, M., Petrou, E., Omma, J., Mattinson, C., Garzanti, E., 2017, QEMSCAN+LAICPMS: a new tool for petrochronology and sedimentary provenance analysis: Geochemistry, Geophysics, Geosystems, in review.

Vincent, P., 2008, Saudi Arabia: an environmental overview: London, Taylor & Francis/Balkema, 309 p.

von Eynatten, H., Pawlowsky-Glahn, V., and Egozcue, J.J., 2002, Understanding perturbation on the simplex: a simple method to better visualise and interpret compositional data in ternary diagrams: Mathematical Geology, v. 34, p. 249-257.

Walkden, G.M., and Williams, A., 1998, Carbonate ramps and the Pleistocene-Recent depositional systems of the Arabian Gulf, *in* Wright, V.P., and Burchette, T.P., eds., Carbonate Ramps: Geological Society of London, Special Pubblication 149, p. 43-53.

Wentworth, C.K., 1919, A laboratory and field study of cobble abrasion: The Journal of Geology, v. 27, p. 507-521.

Williams, A.H., and Walkden, G.M., 2002, Late Quaternary highstand deposits of the southern Arabian Gulf: a record of sea-level and climate change: Geological Society London, Special Publication 195, p. 371-386.

Zuffa, G.G., 1985, Optical analyses of arenites: influence of methodology on compositional results, *in* Zuffa, G.G., ed., Provenance of arenites: Dordrecht Reidel, NATO ASI Series 148, p. 165-189.

Zuffa, G.G., Normark, W.R., Serra, F, and Brunner, C.A., 2000, Turbidite megabeds in an oceanic rift valley recording Jökulhlaups of Late Pleistocene glacial lakes of the western United States: The Journal of Geology, v. 108, p. 253-274.

Fig. 1 Gulf to Rub' al Khali

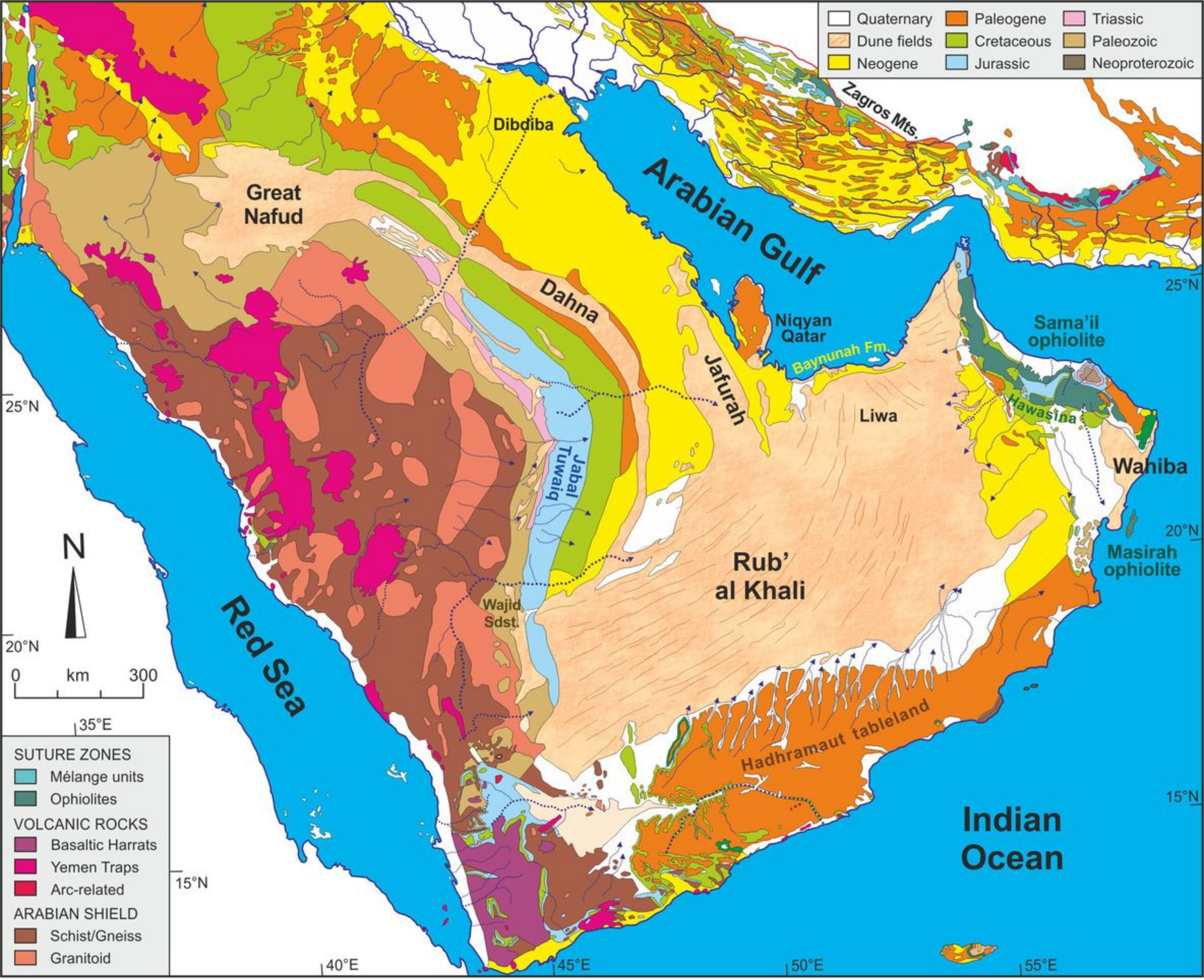

Fig. 2 Gulf to Rub' al Khali

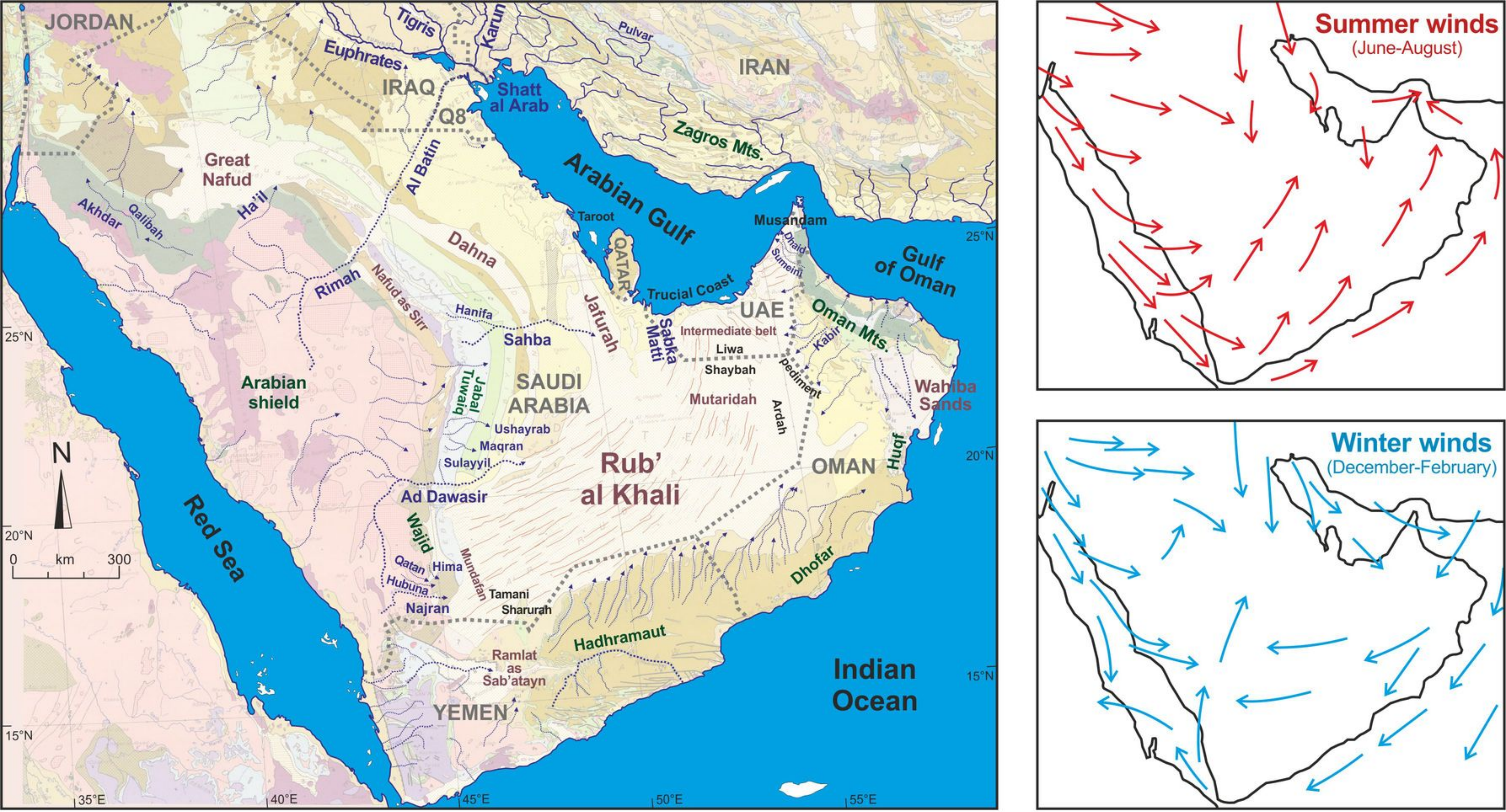

Fig. 3 Gulf to Rub' al Khali

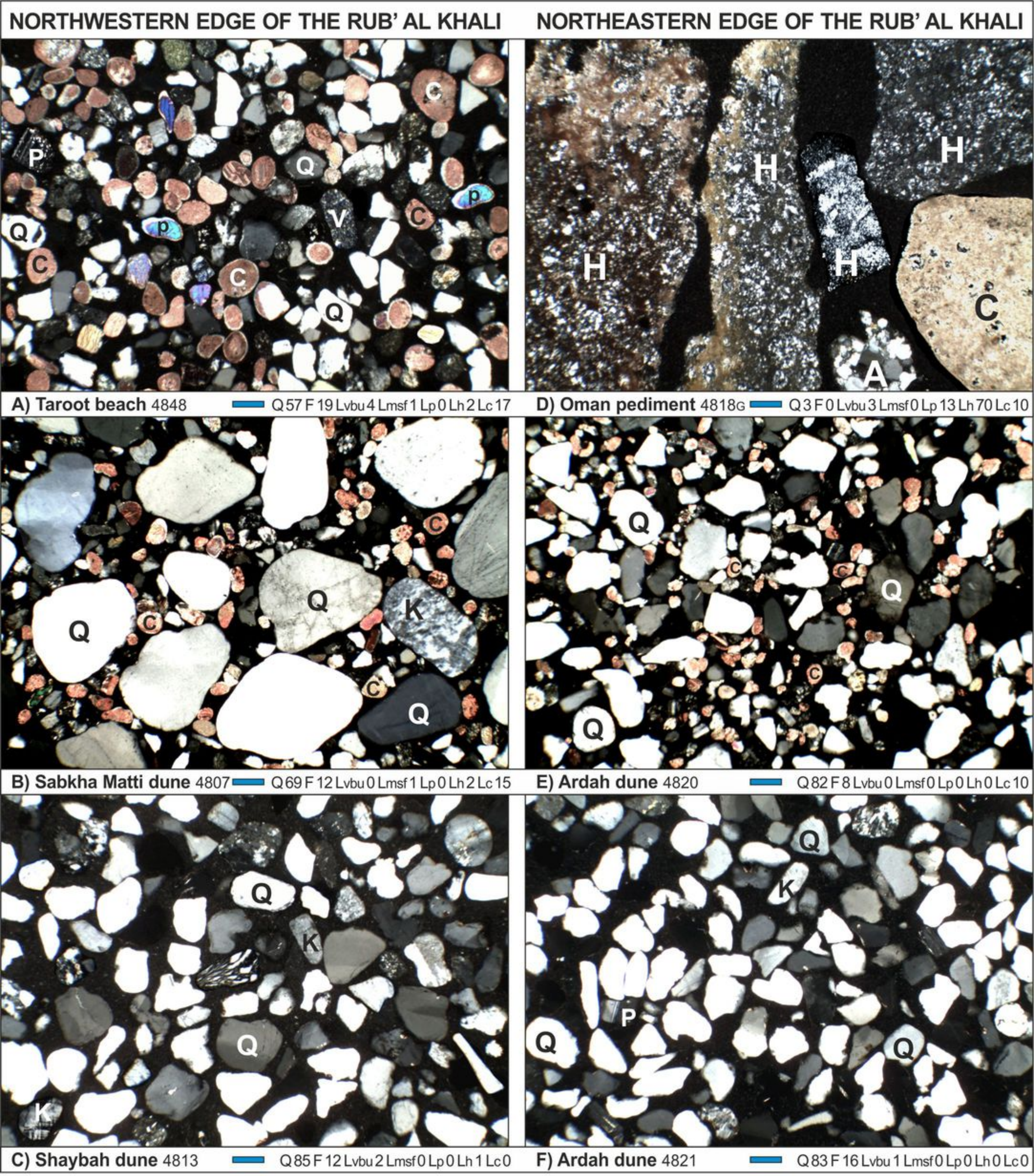

Fig. 4 Gulf to Rub' al Khali

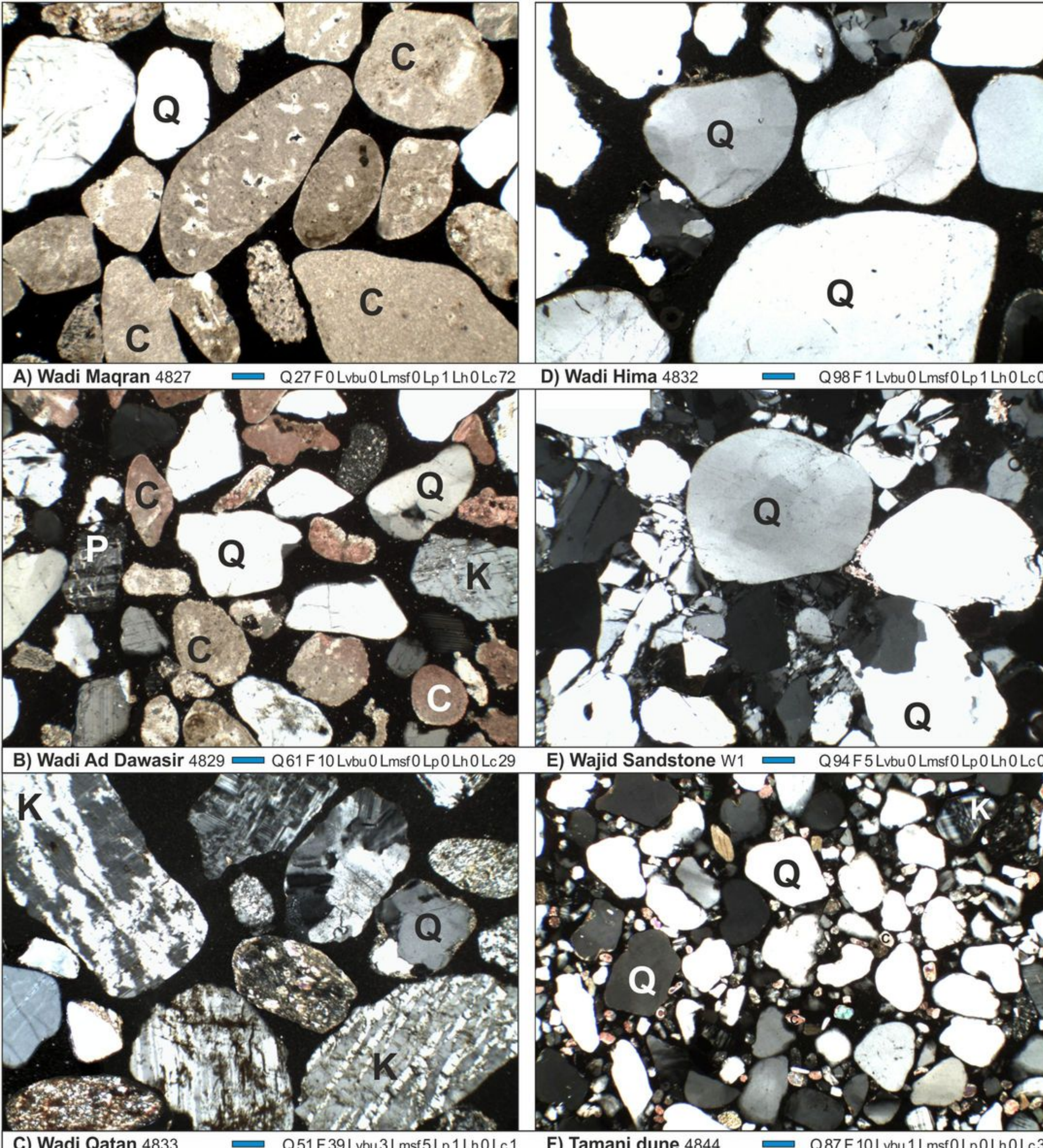

Fig. 5 Gulf to Rub' al Khali

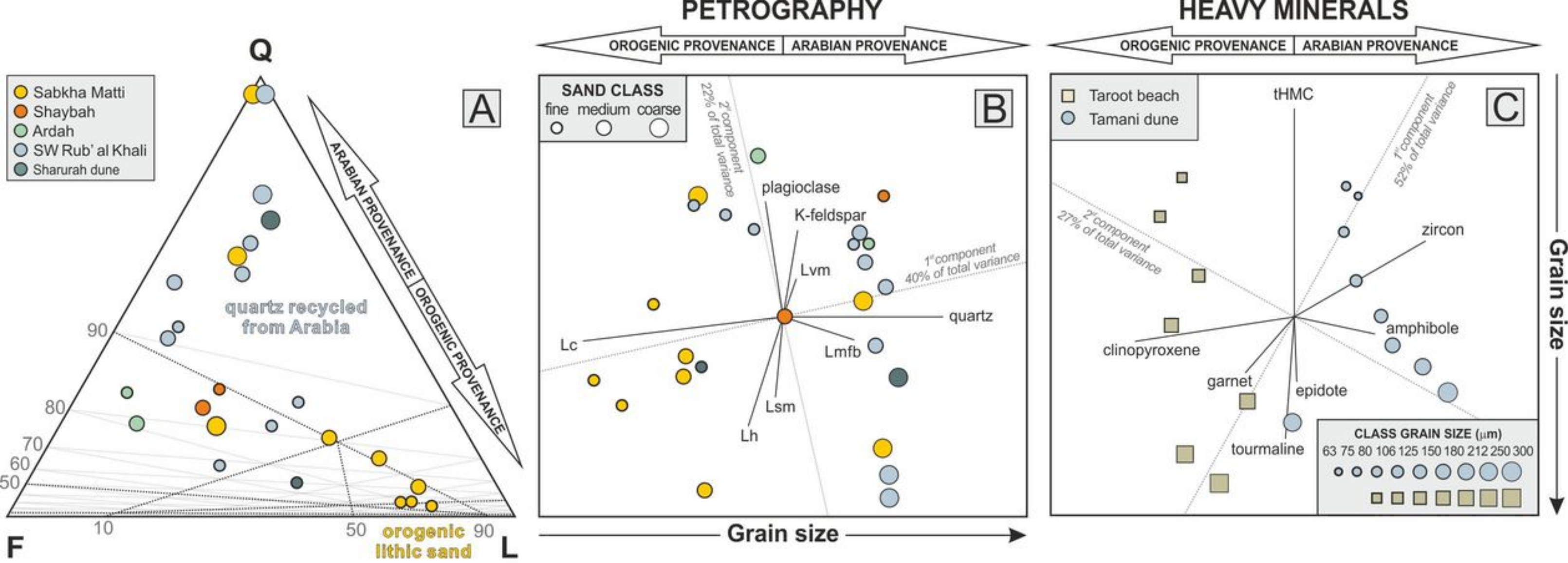

Fig. 6 Gulf to Rub' al Khali

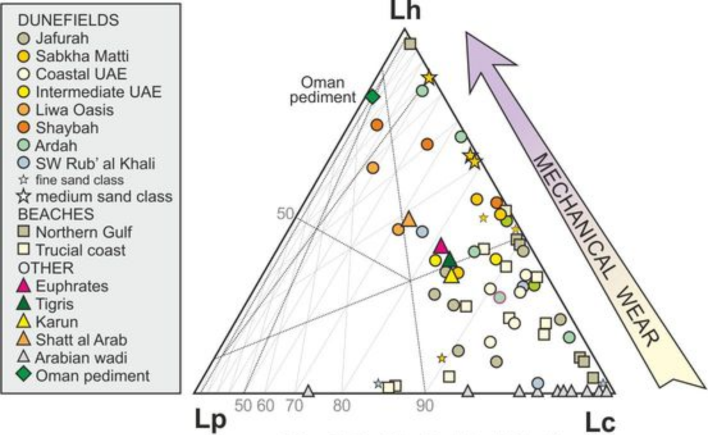

Fig. 7 Gulf to Rub' al Khali

Fig. 8 Gulf to Rub' al Khali

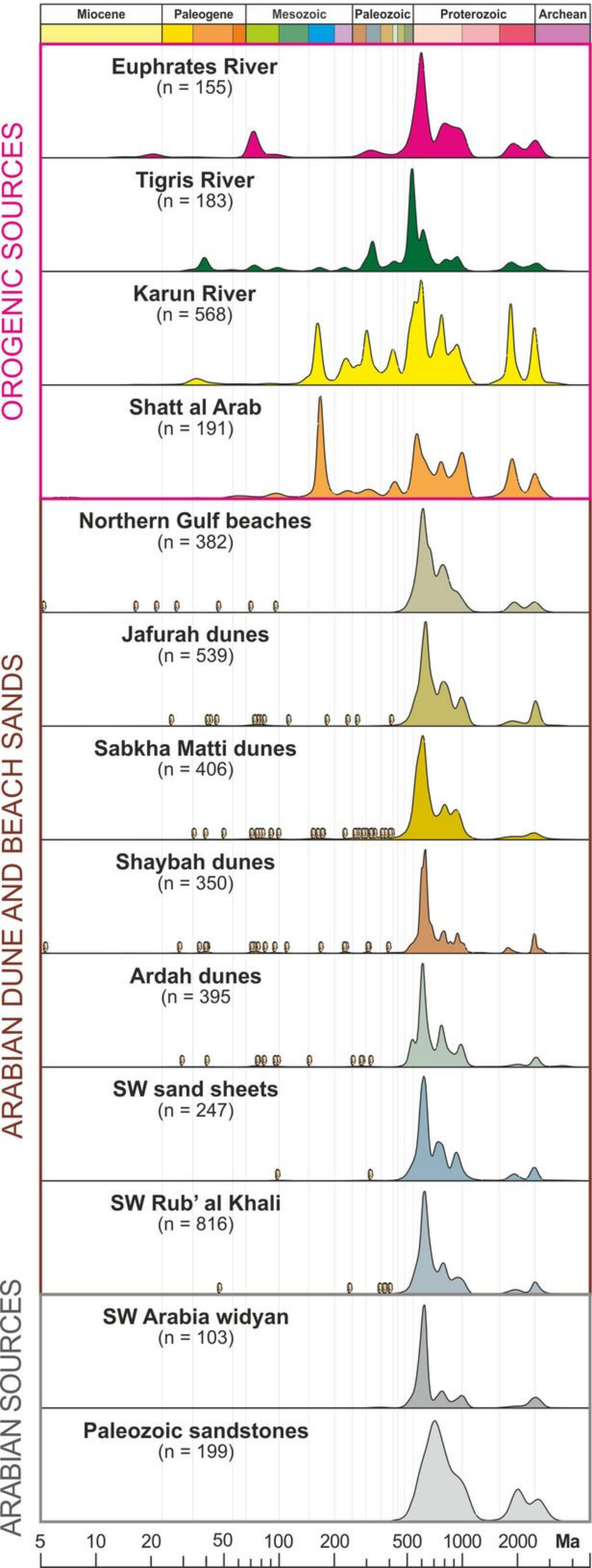

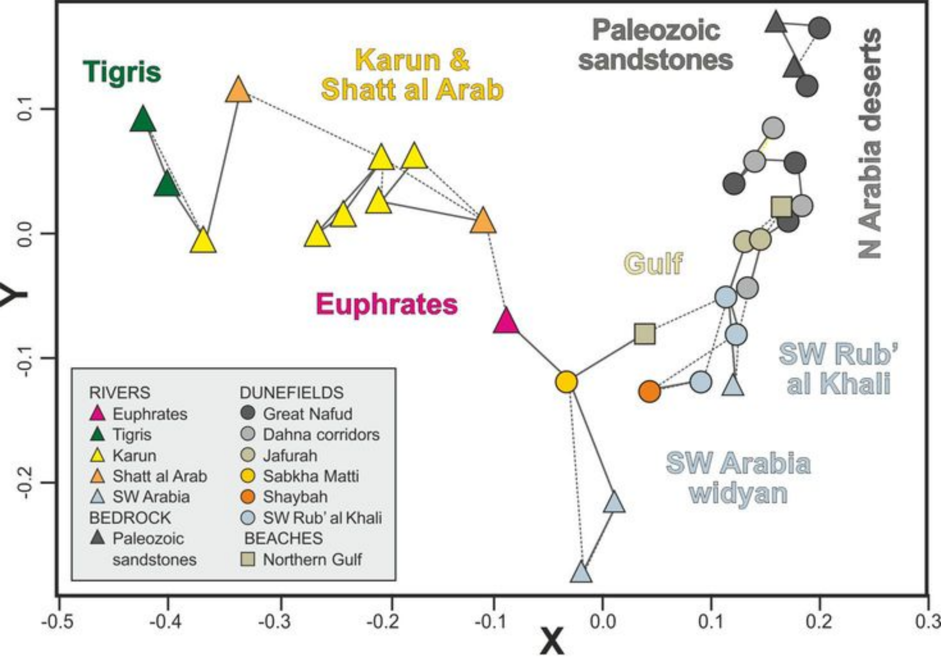

Fig. 9 Gulf to Rub' al Khali

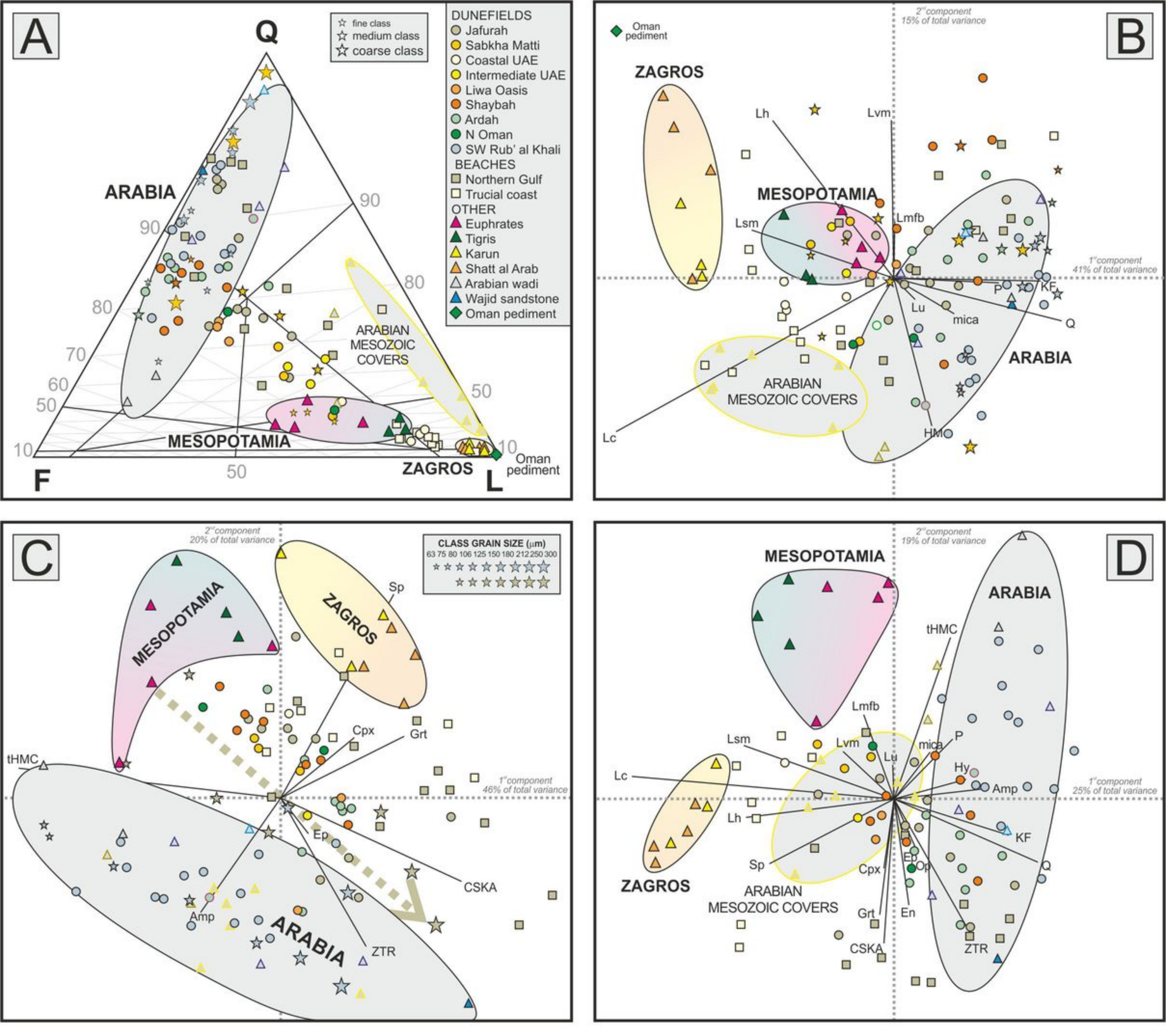

Figure 10 Gulf to Rub' al Khali

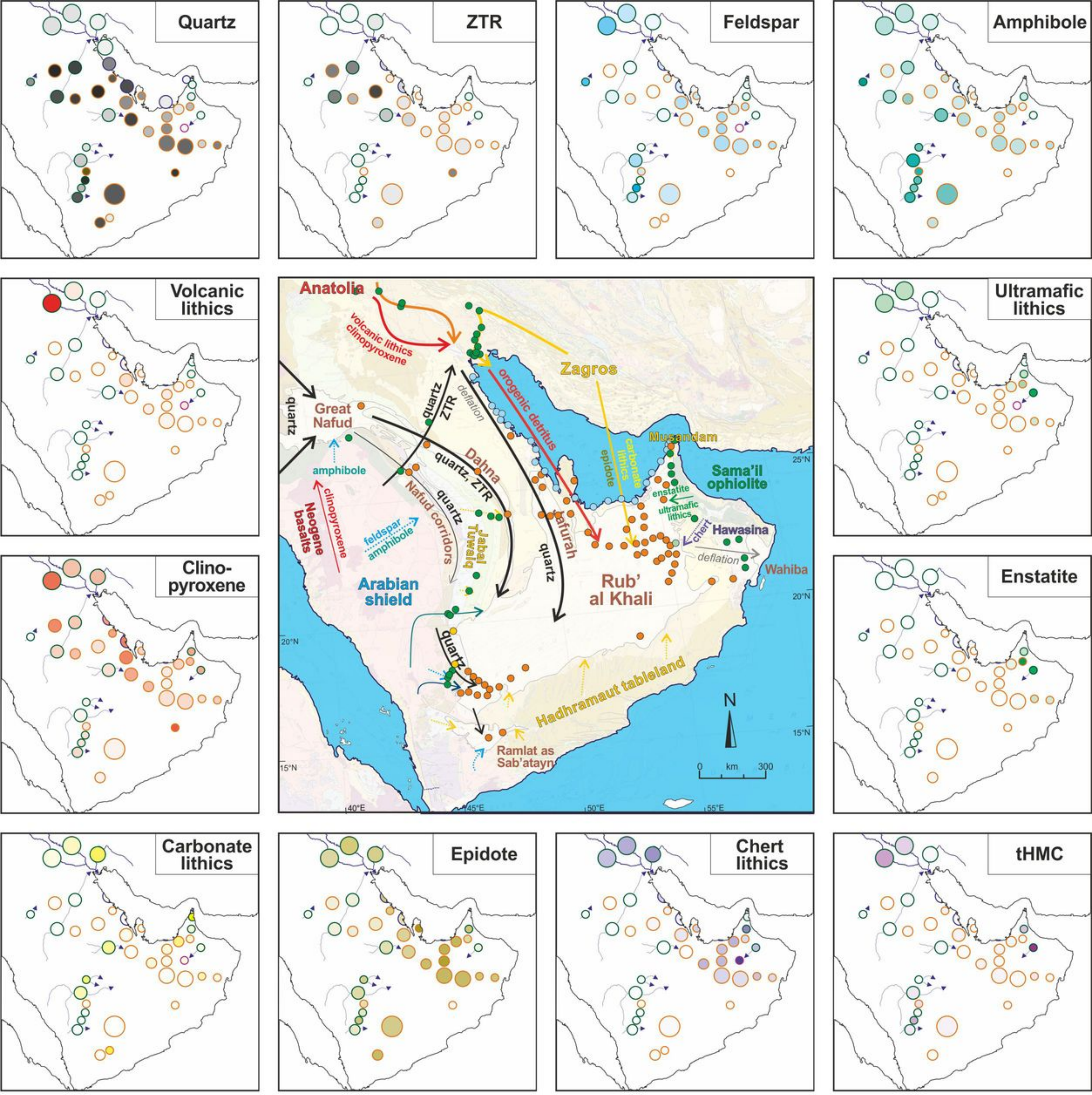

Fig. 11 Gulf to Rub' al Khali

Table 1

	N°	Q	F	Lc	Lh	Lms	Lmv	Lu	mica	HM		P/F	N°	tHMC	ZTR	Ep	Grt	CSKA	Amp	Cpx	En	Hy	Ol	Sp	&tHM	
MESOPOTAMIA																										
Euphrates River	3	30	20	14	2	4	17	4	1	7.7	100.0	.78	3	8.5	0	24	4	1	29	31	0	8	0	1	1	100.0
Tigris River	3	29	10	30	4	11	7	3	2	5.1	100.0	.80	3	4.2	2	36	15	0	26	14	0	0	0	3	3	100.0
Karun River	7	11	4	64	13	6	1	0	0	1.0	100.0	.74	7	0.7	9	35	9	2	18	13	0	0	0	10	3	100.0
Shatt al Arab	4	9	3	60	16	8	3	0	0	0.4	100.0	.63	4	0.3	3	46	7	4	11	21	0	0	0	6	3	100.0
ARABIAN WIDYAN																										
Ha'il	1	70	25	2	0	1	0	0	0	1.7	100.0	.53	1	0.8	4	6	0	0	89	1	0	0	0	0	1	100.0
Rimah/Al Batin	2	92	3	4	0	1	1	0	0	0.3	100.0	.33	2	0.3	42	9	2	0	33	11	0	0	0	0	2	100.0
Sabha/Hanifa	2	45	2	51	0	1	0	0	0	0.2	100.0	n.d.	3	0.5	23	16	1	0	51	7	0	0	0	0	3	100.0
Ushayrab/Maqran	2	27	0	71	0	1	0	0	0	0	100.0	n.d.	2	0.2	11	30	3	1	51	4	0	0	0	0	1	100.0
Sulayyil	1	48	0	48	0	3	0	0	0	0	100.0	n.d.	1	0.6	4	27	1	0	61	2	0	1	0	0	2	100.0
Ad Dawasir	1	46	14	38	0	0	0	0	0	1.1	100.0	.57	2	2.1	4	23	1	0	69	2	0	0	0	0	1	100.0
Hima	1	98	1	0	0	1	0	0	0	0.3	100.0	n.d.	1	0.4	3	16	11	0	58	7	1	1	0	0	2	100.0
Qatan/Hubuna	2	53	32	1	0	5	3	0	2	4.8	100.0	.68	2	7.8	2	35	2	0	50	7	0	2	0	0	2	100.0
Najran	1	88	9	0	0	1	1	0	1	0.3	100.0	.67	1	2.0	2	14	2	1	64	9	0	3	4	0	2	100.0
Oman	8	8	2	24	11	8	3	34	0	11	100.0	.83	4	9.0	2	28	3	0	16	19	18	3	9	2	0.1	100.0
Musandam	2	2	0.2	95	0.2	3	0	0	0	0	100.0	n.d.														
GULF BEACHES																										
Northern Gulf	12	81	8	8	1	0	2	0	0	0.6	100.0	.34	12	0.3	14	29	16	1	13	23	1	1	0	1	2	100.0
Trucial coast	10	19	9	60	3	4	2	1	0	2.1	100.0	.64	7	0.4	3	45	16	1	18	10	5	0	0	1	1	100.0
DUNEFIELDS																										
Dahna-Nafud corridors	6	98	2	0	0	0	0	0	0	0	100.0	.49	6	0.2	42	10	2	0	25	15	0	0	0	0	4	100.0
Jafurah	9	81	10	6	0	1	2	0	0	0.5	100.0	.30	9	0.8	10	27	10	1	23	24	1	1	0	1	4	100.0
Niqyan Qatar	1	72	10	15	1	0	1	0	0	0	100.0	.53	1	0.1	3	62	7	4	12	10	1	0	0	1	1	100.0
Coastal UAE	3	24	9	58	4	2	1	1	0	1.4	100.0	.53	3	0.8	5	43	12	0	22	10	5	1	0	1	1	100.0
Eastern UAE	2	55	11	21	1	2	2	6	0	2.2	100.0	.43	2	1.3	1	24	5	0	11	15	42	1	1	0	0	100.0
Intermediate belt	2	59	14	19	2	3	2	0	0	1.3	100.0	.46	2	0.9	8	46	11	1	27	5	1	0	0	0	1	100.0
Sabkha Matti	3	55	15	20	3	2	3	0	0	2.2	100.0	.54	3	1.2	5	39	14	1	24	16	0	0	0	0	1	100.0
Liwa	2	73	15	6	3	2	1	0	0	1.0	100.0	.48	2	0.4	8	56	15	1	17	2	1	0	0	0	0	100.0
Shaybah	7	81	14	2	1	1	1	0	0	0.2	100.0	.55	7	1.0	6	42	11	1	31	7	0	0	0	1	2	100.0
Ardah	9	85	11	3	1	0	0	0	0	0.6	100.0	.48	8	0.5	7	40	14	1	25	9	1	0	0	0	2	100.0
Oman pediment	1	3	0	10	70	13	3	0	0	0	100.0	n.d.														
Northwest Oman	1	42	15	34	2	1	1	2	1	2.2	100.0	.35	1	2.2	6	35	8	0	25	7	12	1	2	1	2	100.0
Northeast Oman	1	77	12	8	1	1	0	0	0	0.7	100.0	.19	1	0.4	5	34	8	0	28	11	9	0	1	1	0	100.0
South Oman	1	96	0	1	0	3	1	0	0	0.3	100.0	n.d.	1	0.1	40	1	0	0	10	35	0	0	11	1	2	100.0
Sand sheets	2	83	9	3	0	0	0	0	1	3.1	100.0	.57	2	3.1	4	21	0	0	67	5	1	0	0	0	1	100.0
SW Rub' al Khali	12	86	9	1	0	0	1	0	0	1.9	100.0	.52	12	1.2	7	31	4	1	52	3	0	0	0	0	2	100.0
Ramlat Sab'atayn	1	90	3	4	0	1	1	0	0	0.6	100.0	n.d.	1	0.5	14	41	12	3	25	3	3	0	0	1	1	100.0
Hadhramaut	1	21	0	79	0	0	0	0	0	0	100.0	n.d.														
WAJIID SANDSTONE	1	94	5	0	0	0	0	0	0	0.3	100.0	.63	1	0.03	54	9	11	11	9	3	0	0	0	0	3	100.0